

## RESEARCH ARTICLE

# Future extremes of temperature and precipitation in Europe derived from a combination of dynamical and statistical approaches

Maria F. Cardell  | Arnau Amengual | Romualdo Romero | Climent Ramis

Grup de Meteorologia, Departament de Física, Universitat de les Illes Balears, Palma de Mallorca, Spain

## Correspondence

Maria F. Cardell, Grup de Meteorologia, Departament de Física, Universitat de les Illes Balears, 07122 Palma de Mallorca, Spain.  
Email: maria.cardell@uib.es

## Funding information

Conselleria d'Innovació, Recerca i Turisme del Govern de les Illes Balears and the Fons Social Europeu, Grant/Award Number: FPI/1931/2016; Secretaria de Estado de Investigación, Desarrollo e Innovación for Ministerio de Economía, Industria y Competitividad, Grant/Award Numbers: CGL2014-52199-R, CGL2017-82868-R

## Abstract

Most of the nature-related economic costs and human losses in many regions of Europe are due to extreme weather events such as heat waves, cold spells, persistent droughts, heavy precipitation and intense cyclonic wind-storms. Extreme precipitation events are projected by climatic models to become more intense over the continent while droughts might last longer by the end of the century. In dry regions as Southern Europe, soils are predicted to dry out as temperatures and evapotranspiration rise and rain-bearing atmospheric circulations become less frequent. Prospects on the future of climate indices linked to extreme phenomena are herein derived by using observed and model projected daily meteorological data. Specifically, E-OBS high resolution gridded datasets of observed precipitation and surface minimum and maximum temperatures have been used as the regional observed baseline. For projections, the same meteorological variables have been obtained from a set of regional climate models integrated in the European EURO-CORDEX project, considering the RCP8.5 future emissions scenario. A quantile–quantile adjustment has been applied to the simulated regional scenarios to reduce biases in modelled extreme regimes. Results suggest that warm days will substantially increase across Europe, consistently with a decrease of cold nights. An increase in heat wave amplitude is expected across the continent, with South Eastern Europe and the Mediterranean as the most affected regions. In contrast, Northern Europe will undergo the largest decrease in cold spell magnitude. An overall rise in the frequency and volume of heavy precipitations is projected in all seasons, even if the number of dry days is also expected to increase, except in the Baltic countries. Regarding abnormally long dry periods (extreme droughts), we find that the occurrence of episodes would reduce over Europe as consequence of projected increases in length.

## KEYWORDS

climate change in Europe, climate indices, extreme weather events, quantile–quantile adjustment, regional climate models

## 1 | INTRODUCTION

Changes in extreme weather regimes are one of the major concerns worldwide for being the cause of important impacts on natural and anthropogenic systems. The Special Report on Extreme Events (SREX) of the Intergovernmental Panel on Climate Change shows evidences that some changes in extreme phenomenology are as result of the increased anthropogenic greenhouse gas emissions (Field *et al.*, 2012). The assessment of extremes such as droughts, floods and heat waves is generally of most relevance for society, economy and stakeholders (Field *et al.*, 2014). Europe is particularly vulnerable to variations in the frequency and intensity of heat waves, persistent droughts, severe convective storms and flash flooding, and violent cyclonic wind-storms. The analysis of past events provides an extensive number of extremes that inflicted serious damage in the European countries (e.g., Beniston, 2004; Schär *et al.*, 2004 about 2003 heat wave; James *et al.*, 2004; Muchan *et al.*, 2015 about heavy precipitation and flood events). Anthropogenic influences have probably led to an increase in temperature extremes on global scale (Field *et al.*, 2012). This tendency is projected to persist throughout the century (e.g., Kharin and Zwiers, 2000). In the context of global warming, heavy precipitation is likely to become more frequent and intense over most of the mid-latitude land masses by the end of the century (Stocker *et al.*, 2013).

Regional climate models (RCMs) (Giorgi and Mearns, 1999; Wang *et al.*, 2004) have been widely used to assess future impacts of extreme phenomenology across Europe. In the last decade, the availability and reliability of RCM simulations have experienced a rapid growth, thanks to projects such as PRUDENCE (Christensen and Christensen, 2007), ENSEMBLES (Van der Linden and Mitchell, 2009), STARDEX (Goodess *et al.*, 2012), and more recently, CORDEX (Giorgi *et al.*, 2009). There are several studies about temperature extremes based on RCM projections (Beniston *et al.*, 2007; Fischer and Schär, 2009; Jacob *et al.*, 2014; Dosio, 2016). The assessment of future precipitation extremes is also present through numerous recent modelling studies (Casanueva *et al.*, 2016; Schär *et al.*, 2016; Rajczak and Schär, 2017). Climate indices from the Expert Team on Climate Change Detection and Indices (ETCCDI; e.g., Sillmann *et al.*, 2013) and the WMO (Klein Tank *et al.*, 2009) are frequently used for the climate assessment of extreme weather events. However, RCM projections still have important systematic errors associated with too coarse spatial resolution and model parametrizations. The assessment of extreme values from daily climatic data is challenging, since incorrect statistical distributions simulated by a model for a given meteorological variable may

lead to misleading conclusions. Therefore, it is advisable to correct them to obtain reliable results of the simulated properties of the climate system (Stepanek *et al.*, 2016).

In the present work, we assess future changes in multiple extreme events that are most likely to affect Europe in forthcoming decades. A set of climatic indices have been specifically designed to describe and encompass the following extremes: warm days, heat waves, cold nights, cold spells, heavy precipitation days, heavy precipitation episodes, dry days and severe droughts. This set of climatic indices has been derived for the present climate by using the E-OBS gridded dataset so as to test its reliability in describing the extremes of interest. Next, future trends of the climate indices have been obtained from the EURO-CORDEX simulations. On one hand, the novelty of the work relies on the definition of climatic indices specifically focused to characterize extreme phenomena that can entail a high risk for European societies. The idea is to highlight the most likely future vulnerable geographical areas in terms of the impacts of these extreme events as the century progresses. On the other hand, we have applied a statistical approach to correct biases present in the regional climate models. Specifically, the quantile–quantile adjustment by Cardell *et al.* (2019) will be used to correct the errors found in the extremes of the simulated cumulative distribution functions (CDFs).

The rest of the paper is structured as follows: Section 2 describes the observed and simulated databases used and the quantile–quantile correction method; Section 3 introduces the climatic indices used for the definition and quantification of extreme events, and discusses the projected annual and seasonal mean changes for the parameters of interest; finally, Section 4 summarizes the main results and conclusions, offering some additional remarks for future work.

## 2 | DATABASE AND METHODS

### 2.1 | Input data

The observational references come from the European Climate Assessment and Dataset (ECA& D) project which provides the gridded data set E-OBS (Haylock *et al.*, 2008; further information at [www.ecad.eu](http://www.ecad.eu)). E-OBS covers the entire European land surface and it is available at four different spatial resolutions. Here, we use the highest resolution dataset of about 25 km. For the assessment of future extremes of temperature and precipitation, we adopt present climate reference data from E-OBS of 2-m daily minimum and maximum temperatures and accumulated precipitation for the 1981–2005 period (25 years).

Regarding future projections, the same meteorological variables have been obtained from the EURO-CORDEX project (<http://www.euro-cordex.net>). We used a set of 14 RCMs simulations with a spatial resolution of approximately 12 km. This ensemble is composed of 5 RCMs (ALADIN53, CCLM4-8-17, HIRHAM5, RACMO22E, and RCA4) driven by different GCMs under the future emission scenarios RCP4.5 and RCP8.5. The 2021–2095 period was selected for the study of future extreme phenomenology over Europe. It was divided into three successive 25-year time slices: 2021–2045 (early 21st century), 2046–2070 (mid 21st century), and 2071–2095 (late 21st century).

## 2.2 | The quantile–quantile adjustment

The assessment of future extremes of temperature and precipitation requires reliable projections of climatic variables from RCMs. However, RCM outputs typically present strong biases that need to be statistically corrected to obtain meaningful results on the simulated properties of the climate system (Stepanek *et al.*, 2016). Adjustment procedures have been widely used to amend these inaccuracies and provide more reliable model outputs for climate change studies.

Within this context, we apply a Q–Q adjustment specifically focused on the amelioration of the extremes of the distribution. The statistical approach is based on a

non parametric function that corrects mean, variability and shape errors in the simulated CDFs. It can be expressed as the following relationship between the *i*th quantiles (Figure 1): *p<sub>i</sub>* (projected or future calibrated), *o<sub>i</sub>* (control observed or baseline), *s<sub>fi</sub>* (raw future simulated) and *s<sub>ci</sub>* (raw control simulated).

$$p_i = o_i + \alpha \bar{\Delta} + \beta_i \Delta'_i, \tag{1}$$

where

$$\bar{\Delta} = \frac{\sum_{i=1}^N \Delta_i}{N} = \frac{\sum_{i=1}^N (s_{fi} - s_{ci})}{N} = \bar{s}_f - \bar{s}_c, \tag{2}$$

$$\Delta'_i = \Delta_i - \bar{\Delta}, \tag{3}$$

and

$$\text{Precipitation: } \alpha = \frac{\left(\sum_{i=1}^N o_i\right)/N}{\left(\sum_{i=1}^N s_{ci}\right)/N} = \frac{\bar{O}}{\bar{S}_c}$$

$$\text{Temperature: } \alpha = 1 \tag{4}$$

$$\beta_i = \frac{o'_i}{s'_{ci}} = \frac{o_i - \bar{O}}{s_{ci} - \bar{S}_c} \tag{5}$$

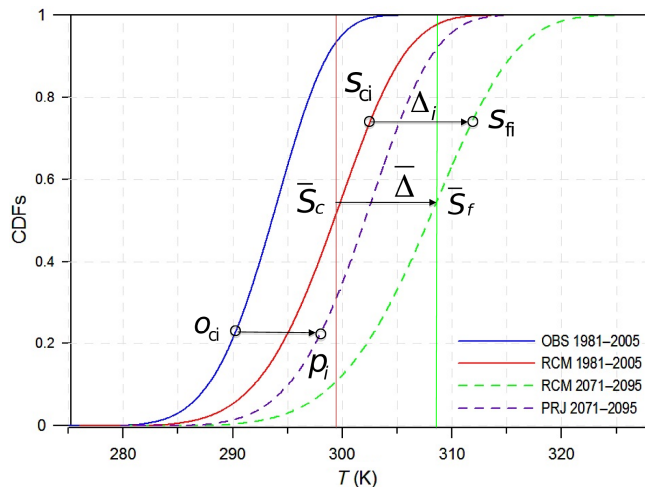


**FIGURE 1** Graphical sketch of the Q–Q adjustment. The CDFs of the mean temperatures are shown for the observed control (OBS 1981–2005), raw control (RCM 1981–2005), and future simulated (RCM 2071–2095) and calibrated or projected (PRJ 2071–2095) data. The statistical correction is illustrated between the 25-year past (1981–2005) and future (2071–2095) periods. Vertical lines denote mean values for raw control (*S<sub>c</sub>*) and future (*S<sub>f</sub>*) simulated periods [Colour figure can be viewed at [wileyonlinelibrary.com](http://wileyonlinelibrary.com)]

The *o<sub>i</sub>'* and *s<sub>ci</sub>'* in Equation (5) are the parametric differences between the observed *i*th quantile and its mean ( $\bar{O}$ ), and the simulated *i*th quantile and its mean ( $\bar{S}_c$ ), respectively. In the equations,  $\Delta_i$  is the difference between future and control raw *i*th quantiles (Figure 1). Accordingly, it can be written as the sum of the mean regime shift ( $\bar{\Delta}$ ) plus the corresponding deviation  $\Delta'_i$  from this shift (Equations (2) and (3)).

The variation in the mean state  $\bar{\Delta}$  is modulated by  $\alpha$  (the scale factor), while  $\beta_i$  (the form factor) calibrates the change in variability and shape expressed by  $\Delta'_i$ . The  $\alpha$  and  $\beta$  parameters are used to fit the RCM in the control period with the observed climate, taking into account the different nature of temperature and precipitation variables (see Cardell *et al.*, 2019 for details).

To build the present climate CDFs, climatic variables from the 25-year observed (E-OBS) and simulated (EURO-CORDEX) baselines (1981–2005) are considered, while future distributions are based on simulated intervals of the same length (i.e., 2021–2045, 2046–2070 and 2071–2095). These future periods were subjected to the Q–Q adjustment approach to build the future calibrated climate change scenarios.

It should be noted that the performance of the calibration method was successfully tested by Cardell *et al.* (2019) through a validation process. Table 1 contains a comparison between ensemble-mean calibrated and raw distributions of daily accumulated precipitation, 2-m minimum and maximum temperatures historical runs against observed CDFs for the 1956–1980 independent period. The Perkins skill score metric (PSS; Perkins *et al.*, 2007) was applied to measure the overlap between raw and calibrated probability density functions (PDFs). Particularly, the PSS associated to the tails of the distributions (i.e., under fifth and over 95th percentiles) was computed to evaluate the performance for extreme regimes. Results show an overall improvement (i.e., PSS closer to 1) of the calibrated versus uncalibrated PDFs (Table 1). In addition, inter-model spread is reduced after calibration.

### 3 | RESULTS

#### 3.1 | Temperature extremes

Changes in extreme temperatures over long observed time series have been described by different authors using data from European stations (e.g., Yan *et al.*, 2002; Klein Tank and Können, 2003; Alexander *et al.*, 2006; Donat *et al.*, 2013; Fonseca *et al.*, 2016). Warm extremes have been increasing and cold extremes decreasing

during the last decades, in agreement with the observed global warming attributed to the human-induced greenhouse gases by the Intergovernmental Panel on Climate Change (Stocker *et al.*, 2013). Several studies evidence an increased occurrence of summer heat waves along the 21st century (e.g., Frich *et al.*, 2002; Beniston and Stephenson, 2004; Schär *et al.*, 2004; Poumadere *et al.*, 2005; Grumm, 2011). These observed tendencies are expected to persist throughout the century according to modelling studies about temperature extremes (Kjellström, 2004; Beniston *et al.*, 2007; Kjellström *et al.*, 2007; Nikulin *et al.*, 2011; Vautard, 2013; Amengual *et al.*, 2014). On the other hand, cold spells are projected to become less intense and frequent in Western Europe, having a significant climate impact (de Vries *et al.*, 2012; Peings *et al.*, 2013).

This section assesses changes in the frequency of very warm days and in the amplitude of heatwaves over Europe. These changes have been computed by comparing the present (1981–2005) and late future (2071–2095) periods under the RCP8.5 emissions scenario. Future European changes in the frequency of very cold nights and the amplitude of cold spells are also inspected. Certainly, RCP8.5 seems to be the most likely emission scenario in the forthcoming decades, unless greenhouse gas mitigation strategies are fully implemented and effective. Future changes have been expressed in terms of the multi-model ensemble mean, while the *SD* among the models quantifies the inter-model variability.

**TABLE 1** Multi-model mean areal average PSS (%) for the 1956–1980 raw and calibrated PDFs for the indicated atmospheric parameters

Precipitation (mm)		Annual	Winter	Spring	Summer	Autumn
Over $P_{95}$	Raw	75.2 ± 9.1	66.3 ± 12.6	68.1 ± 11.0	–	72.2 ± 10.2
	Calibrated	<b>84.1 ± 3.8</b>	<b>75.1 ± 7.9</b>	<b>76.6 ± 7.4</b>	–	<b>77.1 ± 7.3</b>
Over $P_{99}$	Raw	62.0 ± 15.5	51.1 ± 16.8	50.3 ± 15.6	–	55.4 ± 15.6
	Calibrated	<b>73.4 ± 9.0</b>	<b>58.6 ± 14.7</b>	<b>60.1 ± 14.1</b>	–	<b>59.8 ± 14.2</b>
Min. temperature (°C)		Annual	Winter	Spring	Summer	Autumn
Under $P_5$	Raw	60.9 ± 19.7	49.5 ± 22.9	52.0 ± 22.4	36 ± 27.9	57.2 ± 18.8
	Calibrated	<b>76.5 ± 9.6</b>	<b>63.6 ± 17.0</b>	<b>65.0 ± 15.2</b>	<b>71.2 ± 14.0</b>	68.0 ± 12.6
Over $P_{95}$	Raw	46.1 ± 26.4	47.2 ± 26.3	43.4 ± 28.0	35.4 ± 26.9	50.4 ± 23.7
	Calibrated	<b>77.5 ± 9.6</b>	<b>65.7 ± 21.0</b>	<b>71.0 ± 12.7</b>	<b>66.8 ± 14.1</b>	<b>72.0 ± 12.1</b>
Max. temperature (°C)		Annual	Winter	Spring	Summer	Autumn
Under $P_5$	Raw	62.5 ± 15.4	51.8 ± 19.6	49.9 ± 21.2	44.8 ± 23.7	53.2 ± 16.7
	Calibrated	<b>77.9 ± 8.8</b>	<b>64.1 ± 16.3</b>	<b>64.6 ± 15.4</b>	<b>71.9 ± 13.0</b>	<b>66.4 ± 13.0</b>
Over $P_{95}$	Raw	44.4 ± 22.3	38.0 ± 23.5	39.7 ± 23.0	33.5 ± 23.3	51.2 ± 21.9
	Calibrated	<b>77.4 ± 9.8</b>	<b>63.5 ± 23.5</b>	<b>69.6 ± 12.6</b>	<b>66.6 ± 14.9</b>	<b>71.4 ± 12.7</b>

*Note:* Largest values are emphasized in bold. Also shown as ± the *SD* between models. Note that summer results for precipitation are not considered since this season is fully dry in many zones of the domain.

All figures in Section 3 are complemented by summary tables that illustrate the multi-model regional averages and the interannual *SD* of each extreme index for the different European/Mediterranean regions (Figure 2). These tables consider the 25-year present (1981–2005) and the early (2021–2045), mid (2046–2070) and late (2071–2095) future time slices. In addition, the statistical significance of the future changes in the distribution of each extreme indicator has been assessed by applying the Kolmogorov–Smirnov test (Smirnov, 1948) at the 95% level of confidence.

### 3.1.1 | Warm days

A warm day has been defined as the day in which the maximum temperature ( $T_{\max}$ ) is above the 95th percentile ( $T_{\max 95}$ ) calculated from summer days of 1981–2005 baseline (Table 2). In the present work, this definition of warm day is also used as the corresponding threshold in spring and autumn, thus highlighting the severity of these episodes in the shoulder seasons.

In agreement with Kjellström *et al.* (2007), countries of Southern Europe such as Spain, Portugal, France and Italy present the highest 95th percentiles for  $T_{\max}$  in the present (up to 44°C; Figure 3a), while in Central and Northern Europe, the observed percentiles are within 14–32°C. The former countries suffer an important soil moisture deficit in summer that significantly reduces the latent heat exchange between the soil and the lower atmosphere as an effective mechanism for cooling high surface temperatures. The land-atmosphere energy budget interaction is mainly via sensible heat exchanges that promote an increase in air surface temperatures and

extremes (Hirschi *et al.*, 2011). Future trends in summer show that maximum temperatures will exceed the present  $T_{\max 95}$  more than 10% of days throughout the domain by the late 21st century (Figure 3b; Table 3). The most affected regions by the thermal increase will be South Eastern Europe and the Mediterranean. This strong regional signal would be favoured by an intensification of the anticyclonic circulation over Western and Central Mediterranean (Barcikowska *et al.*, 2019). In addition, the warming tendency over Eastern Europe might be associated with a weakening trend of the north-westerly cool Etesian winds (Saaroni *et al.*, 2003). Notably, the fraction of warm days could reach 59% of the whole summer in Central Spain and north-western Italy, and 80% in North Africa and the Middle East countries. Results present a good certainty given the low inter-model *SD* (less than 15% in *SD*, Figure 3c).

Concerning the spring temperature extremes, the largest fraction of days under severe warm conditions are found over North-Eastern Europe (about 1% of days; not shown). At least, this could partially be in response to a reduction in the snow cover (Giorgi and Lionello, 2008). An increased warming of days is expected over all the continent by the late century, being particularly notable in the Scandinavian countries, Russia and Israel (more than 5% of days, Figure 3d; Table 2). Model's uncertainties associated with these shifts are higher in the regions with largest increases (not shown).

In autumn, almost 1% of the present days are warm days in the Mediterranean (not shown). Future trends show that hot extremes will be more frequent by the 2071–2095, especially in Western Europe and the Mediterranean (Figure 3e; Table 3). For most of Spain, Middle East countries and Africa, more than 5% of autumn days

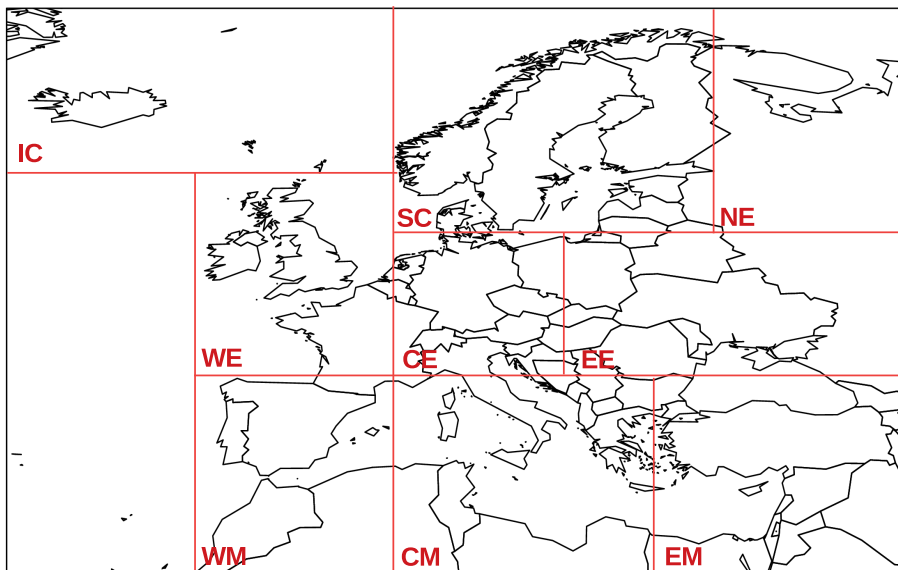


**FIGURE 2** Selected regions of the European/Mediterranean domain: Iceland (IC), Western Europe (WE), Western Mediterranean (WM), Scandinavia (SC), Central Europe (CE), Central Mediterranean (CM), Eastern Europe (EE), Eastern Mediterranean (EM), North-Eastern Europe (NE) [Colour figure can be viewed at [wileyonlinelibrary.com](http://wileyonlinelibrary.com)]

**TABLE 2** Extreme temperature index definitions

Name	Definition	Units
Warm days	Seasonal count when daily max temperature > summer 95th percentile	day
Heat wave	Episode of at least three consecutive days with daily mean temperature > summer 90th percentile	–
Heat wave amplitude	Accumulated heat stress exceedance for all days under heat wave conditions in a given time interval	°C day
Cold nights	Seasonal count when daily min temperature < winter 5th percentile	day
Cold spell	Episode of at least three consecutive days with daily mean temperature < 10th winter percentile	–
Cold spell amplitude	Accumulated cold stress exceedance for all days under cold spell conditions in a given time interval	°C day

will be considered warm with a good agreement among models given the low inter-model *SD* (less than 3% in *SD*, not shown). It must be noted that the observed 95th percentile for  $T_{\max}$  in summer are considerably high in these regions, that is, maximum temperatures of even 44°C in some scattered areas. It is also noting that the projected results differ from the present with a 95% level of confidence throughout the European/Mediterranean regions and seasons (Table 3). These changes would be significant for the three future time slices under the RCP 8.5 scenario. Moreover, the assessment of the interannual variations of warm days across seasons shows that there is a warming trend along the three future periods; the larger the expected changes the greater the interannual variations.

### 3.1.2 | Heat waves

Since heat waves can have different features and effects over a wide range of exposed human groups and areas, it is difficult to stipulate a standard definition. Heat waves have been characterized using several indices, commonly based on a certain period of consecutive days in which weather conditions are excessively warm (e.g., Meehl and Tebaldi, 2004; Beniston *et al.*, 2007; Perkins and Alexander, 2013; Amengual *et al.*, 2014). Adopting absolute thresholds ensures the assessment of extreme events

of a fixed intensity, while geographically relative thresholds guarantee that indices measure episodes of a fixed rarity. Percentile-based thresholds for temperatures are more commonly used since they consider local differences in climatology relative to the area of interest (Beniston *et al.*, 2007; Fischer and Schär, 2010).

In the present work, we consider a heat wave to be an event of at least three consecutive days ( $d_{th} \geq 3$ ) with daily mean temperatures ( $T_{mean}$ ) exceeding the observed summer 90th percentile ( $T_{mean90}$ ; Table 10). The most severe health-related risks results from multi-day heat waves associated with warm nights. Night-time excessive temperatures do not allow the human body to recover from daytime extreme heat stress and aggravate the impact through sleep deprivation (Fischer and Schär, 2010). As a better approach to take into account this type of heat waves, the daily mean temperature has been considered. Heat wave attributes have been characterized with the amplitude exceedance parameter (HWA, Amengual *et al.*, 2014). This attribute is the most relevant to the heat-related risk assessment because it integrates the accumulated stress excess over the entire period under heat wave conditions. Thus, the HWA is the accumulated heat stress exceedance for all days under warm conditions in a given period (Figure 4; Table 2). It is expressed in degrees-day and is specifically defined as:

$$HWA = HWT - T_{mean90} \cdot HWF \quad (6)$$

HWT in Equation (6) denotes the integral of the mean daily temperatures for the whole duration of each individual heat wave, and accumulated for all the heat waves in that period. HWF represents the heat wave day frequency, that is, the number of days under heat wave conditions in the period. Future multi-model mean changes in HWA, compared against the observed time slice (1981–2005), have been analysed for spring, summer and autumn by the late century. Additional results about HWF are also commented, but not displayed.

In the present climate, North-Eastern Europe shows higher summer values of HWA than the Mediterranean (Figure 5; Table 4). Moreover, the observed values of HWF are also higher in North-Eastern Europe (not shown). This fact suggests that there are more consecutive days where  $T_{mean}$  exceeds the observed  $T_{mean90}$ . However, the impact of heat wave amplitude is less serious in terms of human health since the percentiles are quite lower in North-Eastern Europe, ranging from 11 to 23°C instead of 23 to 36°C in the Mediterranean (Figure 5a). That is, heat waves in Northern Europe are characterized by longer periods of relative warm temperatures. In Southern Europe, heat waves are shorter, but more acute and dangerous.

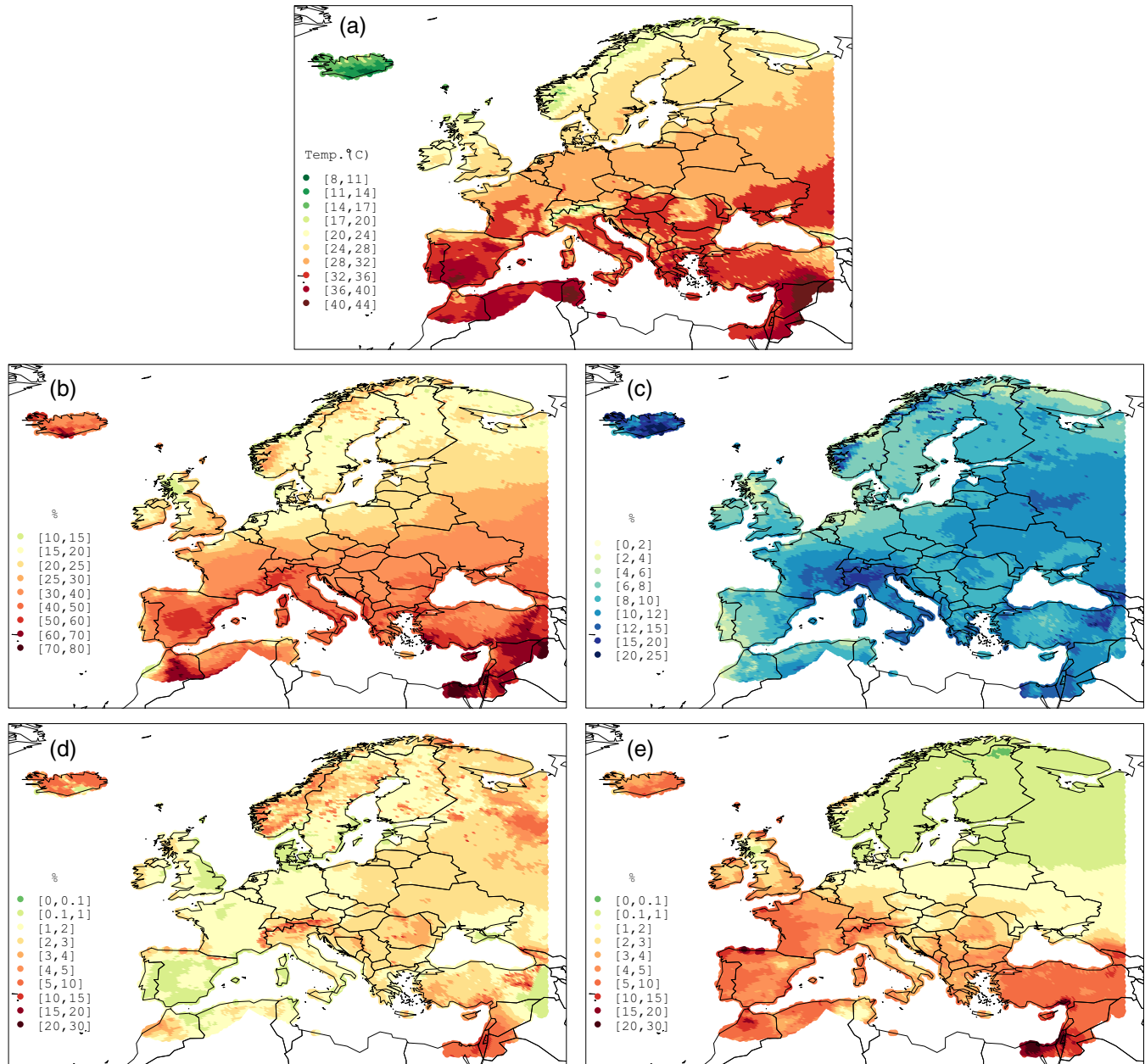


**FIGURE 3** (a) Present observed 95th percentile of daily maximum temperature in summer ( $T_{max95}$ ; 1981–2005) used to define a warm day; (b) future projected percentage of warm days in summer and (c) the corresponding inter-model  $SD$ . Also shown future projected percentage of warm days in (d) spring and (e) autumn [Colour figure can be viewed at [wileyonlinelibrary.com](http://wileyonlinelibrary.com)]

In line with previous findings (Beniston *et al.*, 2007; Fischer and Schär, 2010; Amengual *et al.*, 2014), general increases in the frequency, duration and amplitude of heat waves are expected for all seasons by 2071–2095. South Eastern Europe and the Mediterranean will suffer the largest growth of HWA in summer. This increase may be so disproportionate in response to the combination of anticyclonic weather and amplifying land–atmosphere feedbacks (Vautard, 2013). Indeed, Spain, Northern Africa and some scattered areas of Italy, Greece and Turkey will experience a strong increase of up to 230°C day during the entire summer (Figure 5c). The  $SD$  for the HWA pattern shows a moderate agreement in this

signal among the 14 models, especially in Spain (less than 85°C day in  $SD$ ; Figure 5d). A steady future increase in amplitude exceedance is also projected in North-Eastern Europe and the Scandinavian countries (about 90°C day in average; Table 4), although this result is not very consistent across models ( $SD$  is about 65°C day).

Future changes in heat wave attributes would respond to a different spatial pattern in spring and autumn. In fact, a higher increase in the frequency, duration and amplitude of heat waves might be expected in Northern Europe during spring and in South Eastern Europe and the Mediterranean during autumn. Concerning the spring, some areas of Northern Europe, Italy and

**TABLE 3** Multi-model regional average of warm days (in %) over the European/Mediterranean regions (Figure 2) for present observed (1981–2005) and early (2021–2045), mid (2046–2070) and late (2071–2095) future projected periods

	Spring				Summer				Autumn			
	Present	Early	Mid	Late	Present	Early	Mid	Late	Present	Early	Mid	Late
<b>IC</b>	0.09	<b>0.56</b>	<b>1.58</b>	<b>4.79</b>	5.00	<b>13.36</b>	<b>24.48</b>	<b>43.37</b>	0.20	<b>0.71</b>	<b>2.29</b>	<b>4.97</b>
±	0.34	0.55	0.91	1.53	4.30	3.46	7.48	6.60	0.43	0.42	1.36	1.72
<b>WE</b>	0.10	<b>0.25</b>	<b>0.64</b>	<b>1.47</b>	5.00	<b>9.10</b>	<b>15.68</b>	<b>26.79</b>	0.17	<b>0.73</b>	<b>2.00</b>	<b>4.04</b>
±	0.27	0.25	0.42	0.80	5.32	2.99	4.09	5.54	0.51	0.74	1.03	1.80
<b>WM</b>	0.04	<b>0.14</b>	<b>0.47</b>	<b>1.38</b>	5.00	<b>13.68</b>	<b>26.05</b>	<b>44.82</b>	0.26	<b>0.90</b>	<b>2.51</b>	<b>5.97</b>
±	0.15	0.19	0.43	0.82	4.62	3.31	5.95	6.83	0.71	0.50	1.30	1.87
<b>SC</b>	0.14	<b>0.50</b>	<b>1.04</b>	<b>2.22</b>	5.00	<b>8.23</b>	<b>11.98</b>	<b>19.69</b>	0.01	<b>0.10</b>	<b>0.22</b>	<b>0.50</b>
±	0.42	0.46	0.60	1.05	4.93	2.86	3.26	4.17	0.06	0.16	0.26	0.47
<b>CE</b>	0.06	<b>0.32</b>	<b>0.75</b>	<b>2.25</b>	5.00	<b>11.15</b>	<b>18.44</b>	<b>31.49</b>	0.03	<b>0.36</b>	<b>1.19</b>	<b>3.09</b>
±	0.24	0.34	0.52	1.09	5.69	3.01	4.61	5.89	0.13	0.35	0.79	1.41
<b>CM</b>	0.01	<b>0.15</b>	<b>0.37</b>	<b>1.96</b>	5.00	<b>13.09</b>	<b>25.24</b>	<b>43.44</b>	0.10	<b>0.56</b>	<b>1.13</b>	<b>3.56</b>
±	0.05	0.20	0.31	1.04	5.27	3.07	6.07	7.19	0.33	0.53	0.69	1.34
<b>EE</b>	0.13	<b>0.50</b>	<b>0.96</b>	<b>2.40</b>	5.00	<b>11.08</b>	<b>18.61</b>	<b>32.86</b>	0.05	<b>0.49</b>	<b>0.86</b>	<b>1.95</b>
±	0.39	0.44	0.64	1.16	5.66	3.14	4.13	6.36	0.18	0.52	0.66	0.97
<b>EM</b>	0.19	<b>0.55</b>	<b>1.37</b>	<b>3.68</b>	5.00	<b>15.96</b>	<b>33.06</b>	<b>52.74</b>	0.30	<b>1.48</b>	<b>3.08</b>	<b>7.97</b>
±	0.26	0.32	0.74	1.25	5.48	4.36	6.88	7.47	0.63	1.07	1.42	2.30
<b>NE</b>	0.19	<b>0.66</b>	<b>1.33</b>	<b>2.91</b>	5.00	<b>8.18</b>	<b>11.97</b>	<b>21.72</b>	0.01	<b>0.09</b>	<b>0.17</b>	<b>0.40</b>
±	0.59	0.61	0.79	1.06	5.31	2.38	3.91	4.76	0.07	1.15	0.20	0.38

Note: Significant changes in the future distribution of warm days with respect to the present period, at 95% level of confidence, are emphasized in bold. Also shown as ± the associated interannual SD.

Turkey will suffer an enhanced HWA increase by the late century (up to 60°C day; Figure 5e). In Italy, largest positive changes of HWA occur in the Alps and might be linked to a reduction in the snow cover and the snow-albedo effect (Gobiet *et al.*, 2014). Likewise, Russia and the Middle East will experience amplitude rises between 15 and 30°C day. However, multi-model uncertainties are relatively high in these regions (more than 15°C day in SD, not shown). Finally, it must be noted an important growth rate of HWA along Europe's western coastline and the Mediterranean during the fall (Figure 5f; Table 4). For example, HWA will increase more than 30°C day in Spain, France and United Kingdom coastlines. According to the inter-model SD (not shown), projected results in this case are quite uncertain. Additionally, the analysis of future changes by means of the significance test also points out that projected HWA will differ significantly from the present in all seasons and future periods (Table 4).

### 3.1.3 | Cold nights

Regarding cold temperature extremes, a cold night has been defined as the event in which daily minimum

temperature ( $T_{\min}$ ) is below the observed winter 5th percentile ( $T_{\min 5}$ ; Table 2) from the baseline period (1981–2005). Future trends about cold nights under the RCP8.5 scenario and the SD among models have been displayed for winter in Figure 6.

In agreement with Kjellström *et al.* (2007), present  $T_{\min 5}$  are the lowest in North-Eastern Europe with

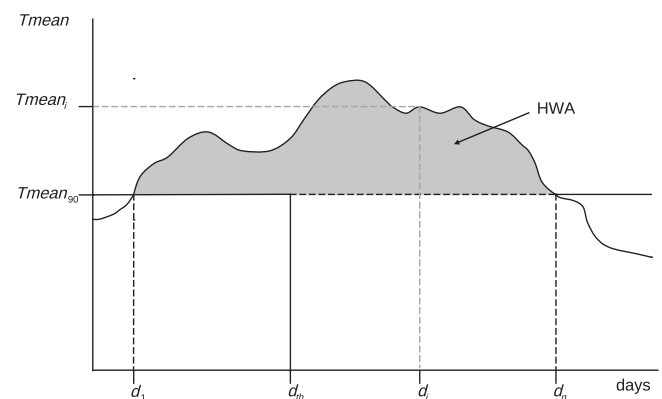


**FIGURE 4** Graphical sketch of heat wave amplitude (HWA, grey shading) exceedances. Note that  $T_{\text{mean}90}$  is expressed in °C and  $d_{\text{th}}$  in days

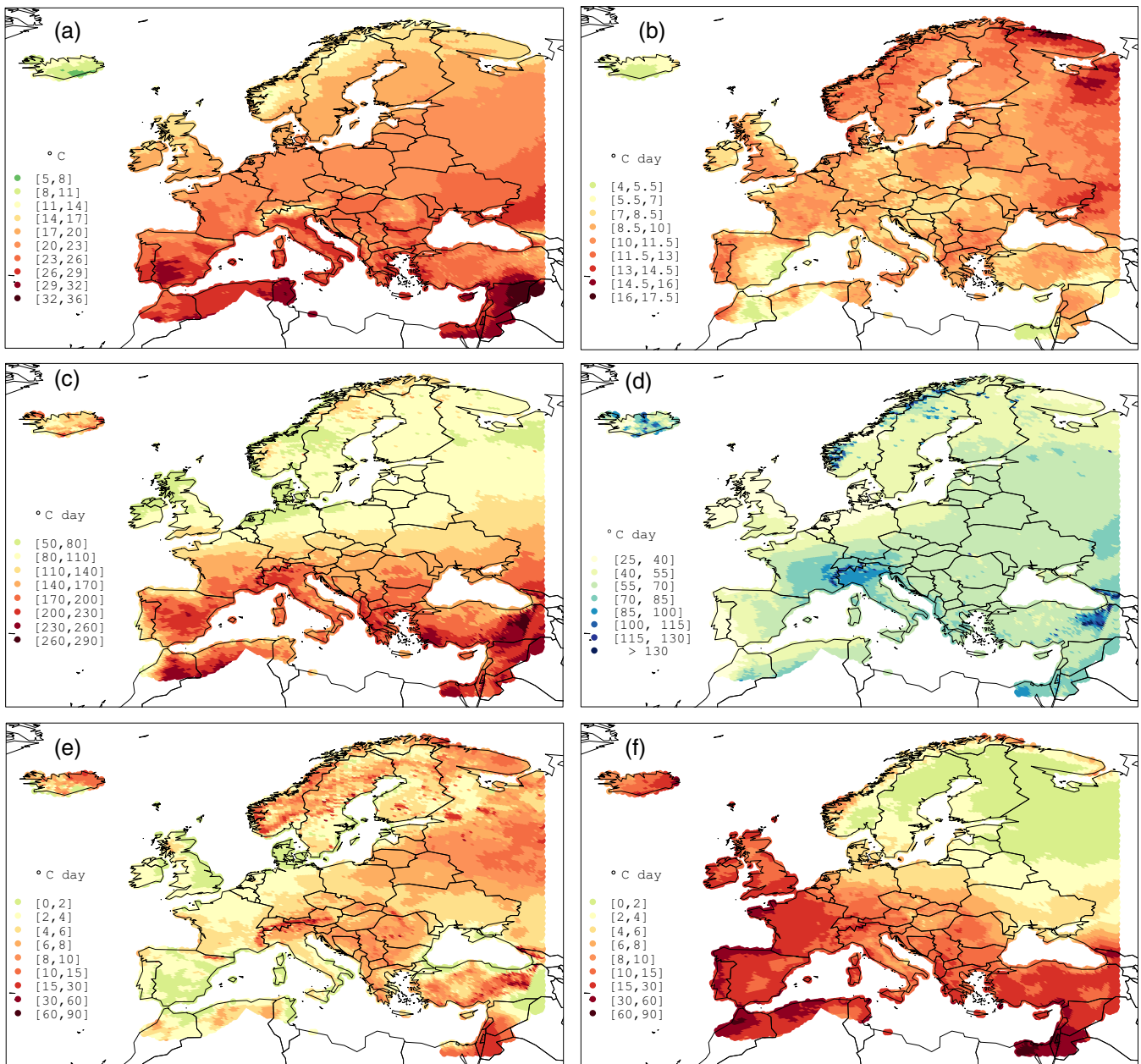


**FIGURE 5** (a) Present observed 90th percentile of daily mean temperature in summer ( $T_{mean90}$ ; 1981–2005), considered for the definition of heat wave amplitude; (b) present observed heat wave amplitude in summer, (c) future change and (d) the corresponding inter-model SD. Also shown future change of heat wave amplitude in (e) spring and (f) autumn [Colour figure can be viewed at [wileyonlinelibrary.com](http://wileyonlinelibrary.com)]

temperatures well below  $-30^{\circ}\text{C}$ , while 5th percentiles are close to  $0^{\circ}\text{C}$  in western maritime and the Mediterranean climates (Figure 6a). Extremely cold temperatures in the former region are usually associated with conditions of clear skies, lands covered with snow and the freezing of soil moisture (Viterbo *et al.*, 1999). Projections would evidence an overall decrease in the percentage of cold nights by the end of 21st century, being particularly intense in Northern Europe. Indeed, hardly 0.2% of the days in winter will be considered as cold nights in the Scandinavian countries and North-Eastern Europe (Figure 6b; Table 5).

The reduction of cold extremes is not so pronounced in Central Europe and the Mediterranean, exhibiting a future percentage of cold nights between 0.4 and 2%. Cold extreme decreases along Western Europe might be favoured by an increase of temperate westerly inflows from the Atlantic ocean (Meehl *et al.*, 2004). Some scattered areas of Spain, Italy, United Kingdom and Turkey will also undergo a strong decrease in the number of cold nights, passing from 5% of days in the present to 0.2% by the late future. It is worth noting that projected results indicate high confidence in these signals

**TABLE 4** As in Table 3, but for heat wave amplitude (in °C day)

	Spring				Summer				Autumn			
	Present	Early	Mid	Late	Present	Early	Mid	Late	Present	Early	Mid	Late
<b>IC</b>	0.01	<b>0.37</b>	<b>1.45</b>	<b>6.58</b>	5.51	<b>23.88</b>	<b>60.76</b>	<b>139.42</b>	0.24	<b>1.14</b>	<b>5.35</b>	<b>15.06</b>
±	0.03	0.60	1.45	3.15	7.83	8.30	23.84	27.20	0.96	0.84	4.04	5.69
<b>WE</b>	0.01	<b>0.22</b>	<b>0.97</b>	<b>3.37</b>	9.51	<b>30.49</b>	<b>62.61</b>	<b>130.16</b>	0.16	<b>2.00</b>	<b>6.94</b>	<b>18.55</b>
±	0.05	0.38	0.93	2.80	14.24	11.86	19.01	33.39	0.64	2.25	4.06	8.83
<b>WM</b>	0.01	<b>0.10</b>	<b>0.63</b>	<b>2.97</b>	8.04	<b>37.66</b>	<b>90.36</b>	<b>193.89</b>	0.27	<b>2.42</b>	<b>8.84</b>	<b>25.26</b>
±	0.07	0.24	0.87	2.29	10.85	11.57	26.88	40.39	0.92	1.46	4.71	8.56
<b>SC</b>	0.04	<b>0.60</b>	<b>1.81</b>	<b>5.95</b>	10.75	<b>25.96</b>	<b>48.04</b>	<b>102.03</b>	0.00	<b>0.22</b>	<b>0.67</b>	<b>2.42</b>
±	0.17	0.98	1.79	4.15	13.44	10.40	16.09	25.16	0.01	0.46	1.01	2.42
<b>CE</b>	0.02	<b>0.45</b>	<b>1.16</b>	<b>6.00</b>	9.06	<b>32.84</b>	<b>65.20</b>	<b>145.20</b>	0.04	<b>0.74</b>	<b>3.06</b>	<b>10.81</b>
±	0.07	0.70	1.23	4.35	13.78	11.27	19.50	35.66	0.18	0.84	2.41	5.44
<b>CM</b>	0.00	<b>0.20</b>	<b>0.66</b>	<b>5.35</b>	9.64	<b>39.37</b>	<b>92.51</b>	<b>194.13</b>	0.02	<b>1.35</b>	<b>3.83</b>	<b>14.61</b>
±	0.00	0.37	0.71	3.25	12.33	11.44	27.05	42.82	0.10	1.43	2.49	5.56
<b>EE</b>	0.06	<b>0.65</b>	<b>1.79</b>	<b>6.51</b>	10.18	<b>32.93</b>	<b>67.30</b>	<b>147.49</b>	0.00	<b>0.73</b>	<b>1.88</b>	<b>5.77</b>
±	0.23	0.84	1.71	4.16	13.47	11.22	18.49	35.96	0.02	1.04	1.88	3.26
<b>EM</b>	0.07	<b>0.47</b>	<b>2.06</b>	<b>8.63</b>	8.60	<b>43.16</b>	<b>109.29</b>	<b>215.58</b>	0.16	<b>2.59</b>	<b>7.03</b>	<b>23.18</b>
±	0.21	0.54	1.74	3.87	11.52	13.93	29.42	44.59	0.48	2.50	4.32	8.46
<b>NE</b>	0.07	<b>1.07</b>	<b>3.01</b>	<b>8.20</b>	11.74	<b>24.60</b>	<b>45.72</b>	<b>104.65</b>	0.00	<b>0.12</b>	<b>0.35</b>	<b>1.42</b>
±	0.32	1.55	3.35	4.97	14.26	7.96	18.35	29.02	0.00	0.31	0.61	1.47

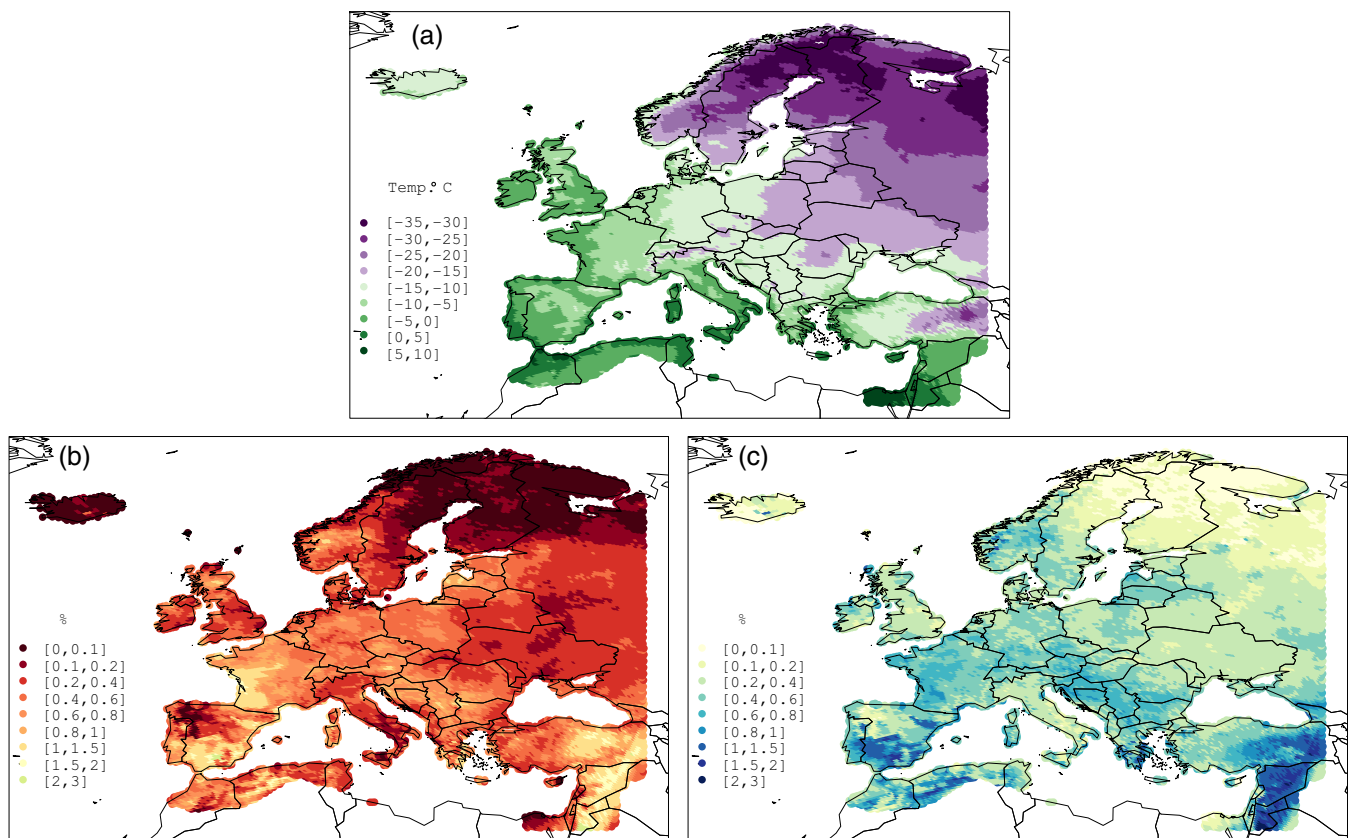


**FIGURE 6** (a) Present observed 5th percentile of daily minimum temperature in winter ( $T_{min5}$ ; 1981–2005) used to define a cold night; (b) future projected percentage of cold nights in winter and (c) the corresponding inter-model SD [Colour figure can be viewed at [wileyonlinelibrary.com](http://wileyonlinelibrary.com)]

**TABLE 5** As in Table 3, but for cold nights (in %)

	Present	Winter		
		Early	Mid	Late
<b>IC</b>	5.00	<b>1.44</b>	<b>0.64</b>	<b>0.06</b>
±	3.65	0.70	0.55	0.08
<b>WE</b>	5.00	2.64	<b>1.46</b>	<b>0.67</b>
±	5.74	1.43	0.98	0.52
<b>WM</b>	5.00	<b>2.74</b>	<b>1.42</b>	<b>0.71</b>
±	5.10	1.28	0.89	0.47
<b>SC</b>	5.00	2.09	<b>0.90</b>	<b>0.28</b>
±	6.46	1.28	0.63	0.28
<b>CE</b>	5.00	2.75	<b>1.30</b>	<b>0.56</b>
±	5.79	1.52	0.87	0.52
<b>CM</b>	5.00	<b>2.63</b>	<b>1.10</b>	<b>0.49</b>
±	4.88	1.25	0.69	0.41
<b>EE</b>	5.00	2.80	<b>1.10</b>	<b>0.39</b>
±	5.92	1.53	0.83	0.47
<b>EM</b>	5.00	<b>2.76</b>	<b>1.41</b>	<b>0.80</b>
±	5.45	1.23	0.89	0.65
<b>NE</b>	5.00	2.00	<b>0.71</b>	<b>0.21</b>
±	5.86	1.35	0.68	0.28

according to the low inter-model *SD*, especially in the regions where the largest decreases are found (Figure 6c). Note that the future percentage of cold nights would be significantly different with respect to the present over all the regions from mid century (Table 5). In addition, the interannual variability is predicted to decrease, despite the large expected change in the percentage of cold nights.

### 3.1.4 | Cold spells

Changes in cold spells could have a significant impact over Europe. An interesting point is to determine whether these episodes will suppose such a cold-related risk as the present-day. We consider a cold spell to be an event of at least three consecutive days ( $d_{th} \geq 3$ ) with mean temperatures under the observed winter 10th percentiles ( $T_{mean}$ ; Table 2). Analogously to the heat wave definition, mean temperature is used to define cold spells as it represents thermal exposure throughout the whole day, while minimum and maximum temperatures only reflect the exposure for a short time period. In addition, mean temperatures give the best model fit with respect to their effects on cause-specific mortality as judged by quasi-Poisson Akaike Information Criterion (Q-AIC; Guo *et al.*, 2012). Again, cold spells have been characterized by the amplitude exceedance. That is, the cold spell

amplitude (CSA) represents the accumulated cold stress exceedance for all days under extreme conditions in a given period (Table 2). It is expressed in degrees-day and specifically defined as:

$$CSA = T_{mean10} \cdot CSF - CST \quad (7)$$

CST denotes the integral of the mean daily temperatures over the duration of each individual cold spell, and accumulated for all the cold spells in that period. CSF represents the cold spell frequency expressed as the number of days under cold spell conditions in this interval.

In the present climate, the cold spells of higher amplitude occur in the Scandinavian countries and North-Eastern Europe (Figure 7; Table 6). These cold spells are more persistent since they present more continuous days with mean temperatures below the  $T_{mean10}$ . In the Mediterranean, cold spells are not so persistent and they are associated with occasional cold polar intrusions, lasting only a few days. Generally, they do not feature a strong impact on health, since  $T_{mean10}$ s are much higher than in Northern Europe (Figure 7a).

Cold spells are projected to be less frequent and severe in Western Europe by the late century (Peings *et al.*, 2013). According to our results, models

**TABLE 6** As in Table 3, but for cold spell amplitude (in °C day)

	Present	Winter		
		Early	Mid	Late
<b>IC</b>	9.79	<b>2.19</b>	0.96	<b>0.08</b>
±	11.93	1.47	1.12	0.19
<b>WE</b>	17.09	10.35	6.81	<b>2.39</b>
±	26.57	6.07	7.22	2.15
<b>WM</b>	10.85	7.63	3.78	<b>1.33</b>
±	13.43	4.65	3.47	1.18
<b>SC</b>	26.54	11.02	4.74	<b>1.26</b>
±	41.57	7.97	4.10	1.50
<b>CE</b>	19.97	11.74	6.63	<b>2.18</b>
±	29.54	7.28	7.31	2.33
<b>CM</b>	12.82	8.45	3.33	<b>1.19</b>
±	15.21	4.44	3.07	1.26
<b>EE</b>	22.93	14.05	6.15	<b>1.79</b>
±	32.57	7.99	6.32	2.21
<b>EM</b>	15.06	8.98	3.72	<b>1.71</b>
±	18.52	4.86	2.88	1.93
<b>NE</b>	30.48	13.98	5.80	<b>1.64</b>
±	44.49	10.34	5.79	2.15

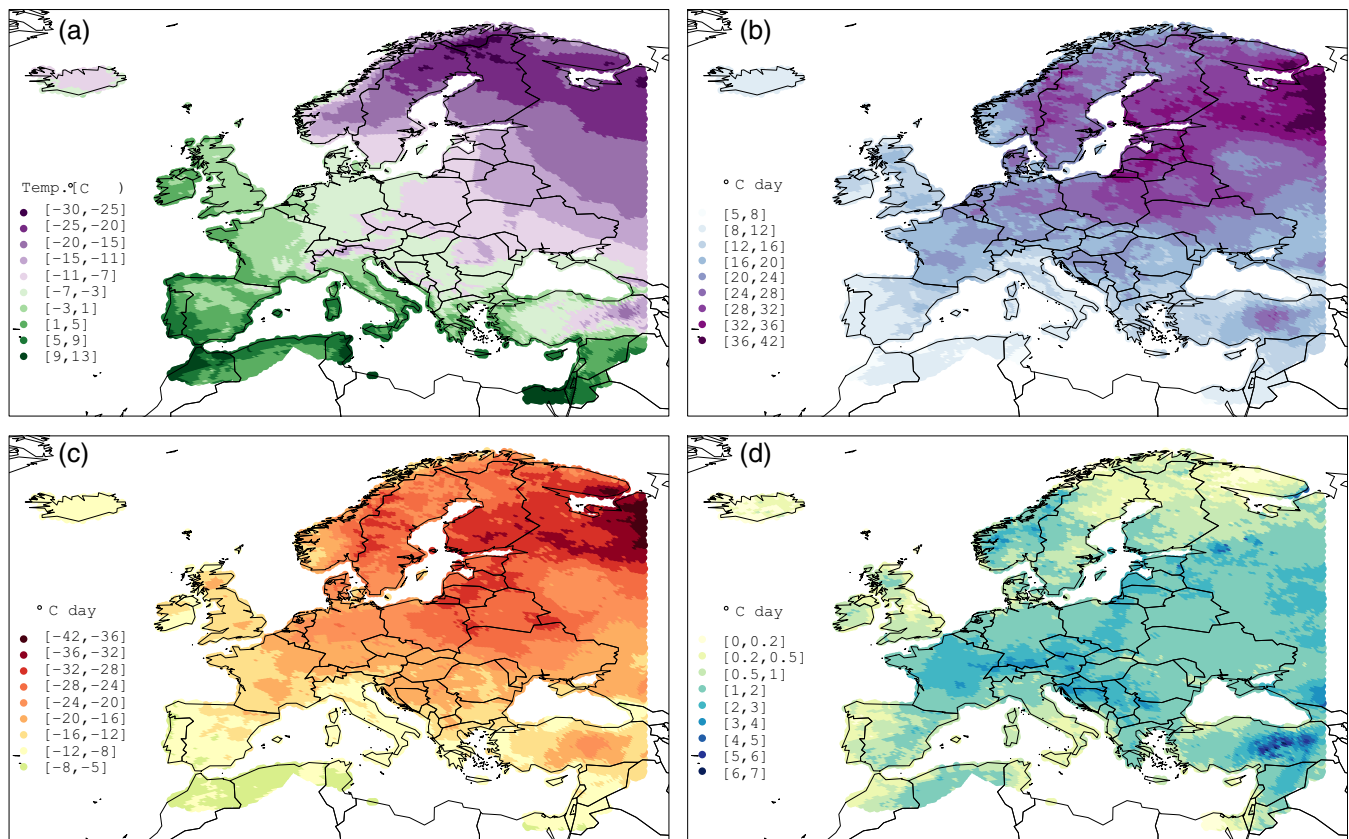


**FIGURE 7** (a) Present observed 10th percentile of daily mean temperature in winter ( $T_{mean10}$ ; 1981–2005) considered for the definition of cold spell amplitude; (b) present observed cold spell amplitude in winter, (c) future change and (d) the corresponding inter-model  $SD$  [Colour figure can be viewed at [wileyonlinelibrary.com](http://wileyonlinelibrary.com)]

consistently project an overall decrease of the CSF and CSA, which is particularly strong in Northern Europe. It must be noted that  $T_{mean10}$ s are between  $-20$  and  $-30^{\circ}\text{C}$  in the Scandinavian countries and North-Eastern Europe (Figure 7a), while present CSA is up to  $30^{\circ}\text{C}$  day (Figure 7b; Table 6). Indeed, CSA of these regions will considerably decrease by an amount in excess of  $30^{\circ}\text{C}$  day (Figure 7c), with a high consistency among models (less than  $1.5^{\circ}\text{C}$  day in  $SD$ ; Figure 7d). Likewise, Central Europe, the Balkans and the interior of Turkey will suffer a significant decrease around  $20^{\circ}\text{C}$  day by 2071–2095. This result is not so consistent across models. A possible contribution to the expected decrease of CSA over Western and Central Europe would be a weakening of the responsible circulation pattern in winter; in addition, a stronger anticyclonic anomaly over the Mediterranean Sea could also enhance the advection of warm air from north Africa and south Atlantic towards Western Europe (Peings *et al.*, 2013). The robustness test of future changes in CSA evidences that the projected average results would be only significant by late century (Table 6).

### 3.2 | Precipitation extremes

Changes in the European hydrological cycle may have substantial impacts on environmental and anthropogenic systems. Modelling studies indicate an intensification of heavy and extreme precipitation events across the continent, while dry days and droughts are projected to increase in Southern Europe throughout the 21st century (Giannakopoulos *et al.*, 2009; Rajczak and Schär, 2017). The climatology of heavy precipitation events and its changes has been described through numerous indices recommended by several initiatives (e.g., WMO; Klein Tank *et al.*, 2009 and ETCCDI (Zhang *et al.*, 2011)). All/wet-day percentiles and mean annual maximum 1–5 days aggregated precipitation are some examples used for the assessment of potential changes in heavy rainfall (Rajczak *et al.*, 2013; Kendon *et al.*, 2014; Ban *et al.*, 2015; Schär *et al.*, 2016; Rajczak and Schär, 2017).

In the present section, several diagnostics of precipitation extremes have been applied across Europe. Projected shifts in heavy precipitation and dry days have been analysed seasonally by means of wet day percentiles and

thresholds. Likewise, the study of heavy precipitation episodes and droughts has been carried out by using different quantitative indicators.

### 3.2.1 | Heavy precipitation days

A heavy precipitation day (HPD) has been defined as an event in which daily accumulated precipitation values are in excess of the observed annual 95th percentile (*Precip95*; Table 7). Therefore, HPD quantifies extreme rainfall which can be directly responsible for floods and soil erosion. Note that *Precip95* has been computed considering only the total number of days with daily accumulated precipitation  $\geq 0.1$  mm (i.e., wet days). Present HPDs are displayed as the seasonal percentage distribution (i.e., with the four seasons adding up to 5%) rather than through the absolute number of days per season. Future changes have been correspondingly expressed as the shifts in these percentages.

It is worth noting that annual precipitation extremes are particularly significant in Southern Europe with values above 40 mm in some spots of areas of the Iberian Peninsula, the Alpine region and the European Mediterranean coastal areas (Figure 8a). Annual precipitation extremes are not so intense in North-Eastern Europe, with amounts ranging from 8 to 20 mm. The former

regions are characterized by deep convection during the extended warm season that results in heavy precipitation lasting for a few hours. These heavy rainfalls account for an important fraction of the total annual amounts. North-Eastern regions are generally more affected by stratiform-like systems, which are characterized by light to moderate rainfall rates lasting over longer time periods.

In the present climate, heavy precipitation days respond to a characteristic geographical distribution depending on the season. In winter, HPDs are more frequent in Southern and western maritime Europe due to the impinging of moist flows associated to Atlantic lows (Figure 8b). In summer, the storm track shifts northwards, mainly affecting the northernmost part of the continent, while in the central countries convective precipitation events are frequent (Figure 8d). In spring and autumn, HPDs are more evenly distributed throughout the domain, being more frequent during the fall (Figure 8c, e). In this season, the Western and Central Mediterranean coastal areas are under the influence of cold air intrusions at upper levels combined with relative warm sea surface temperatures, resulting in deep convection and heavy precipitation.

Models consistently project an increase of precipitation extremes in Central and Northern Europe, while decreasing in some areas of the Mediterranean throughout all the seasons (Figure 9; Table 8). In line with Rajczak and Schär, 2017, the largest positive changes of HPDs are projected in winter and autumn across large parts of Europe by 2071–2095 (Figure 9). This increase might be related to an intensification of the hydrological cycle associated with a growth of atmospheric moisture content (Schmidli *et al.*, 2007). The statistical assessment indicates that projected increases in northern Europe might be significant throughout all the seasons from mid century, while the expected decreases in the Mediterranean would be only significant in summer and autumn (Table 8).

In winter, projections point out an increase of HPDs across most of the domain which is similar to the pattern of change for mean precipitation (e.g., Jones *et al.*, 2001; Cardell *et al.*, 2019). It must be noted a positive growth up to 1.5% in United Kingdom, northern France and countries of middle-west Europe (Figure 9a). However, results include a possible decrease in HPDs between 1 and 2% over Southern Spain, the Atlas and Middle East countries, accompanied by regional increases in parts of Spain and Portugal. The geographical location of the Iberian Peninsula, between tropical and middle latitudes, may be one of the causes of its vulnerability as it could be affected by less frequent Atlantic front passages and more persistent Azores anticyclonic conditions (Casanueva

**TABLE 7** Extreme precipitation index definitions

Name	Definition	Units
Heavy precipitation days	Seasonal count when daily precipitation > annual 95th percentile	day
Heavy precipitation episode	Episode of at least two consecutive days with daily precipitation > annual 95th percentile	–
Heavy precipitation amplitude	Accumulated rainfall stress exceedance for all heavy precipitation days	mm day
Dry days	Annual and seasonal count when daily precipitation < 0.1 mm	day
Dry spell	Episode of at least three consecutive days with daily precipitation < 0.1 mm	–
Drought	Dry spell of length > 95th length percentile of all identified dry spells in the present climate	–

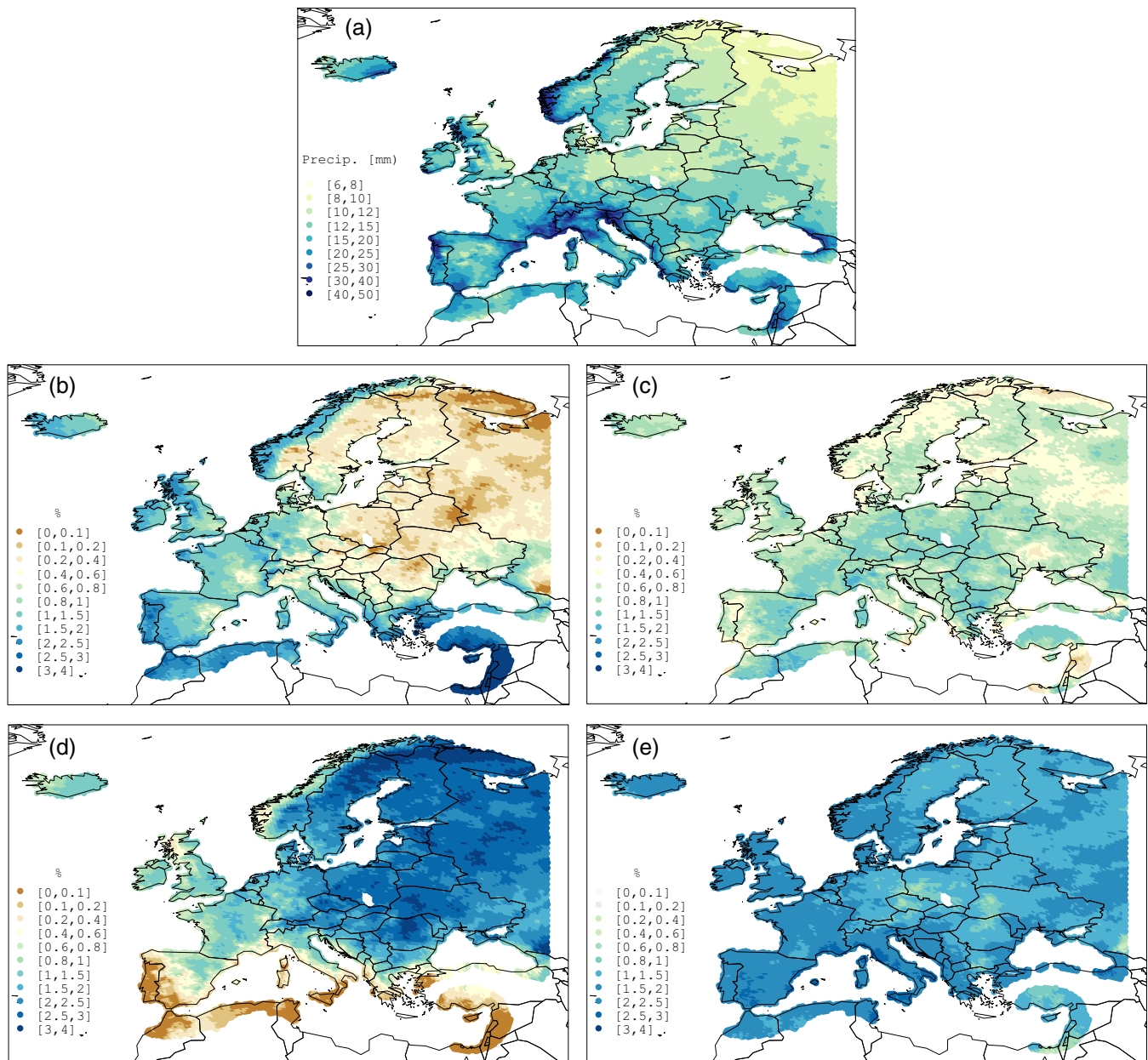


**FIGURE 8** (a) Present observed 95th percentile of daily precipitation, considering the whole year and only wet days (*Precip95*; 1981–2005). This threshold is used to define a heavy precipitation day. Present percentage of observed heavy precipitation days in (b) winter, (c) spring, (d) summer and (e) autumn [Colour figure can be viewed at [wileyonlinelibrary.com](http://wileyonlinelibrary.com)]

*et al.*, 2014). Model's uncertainties associated with these shifts are small in all the domain, showing a robust agreement among models (less than 1% in *SD*, not shown).

Concerning spring, future changes of HPDs present a similar geographical distribution to winter, but these changes are significantly higher in north Europe (Figure 9b; Table 8). For example, HPDs will increase up to 1% in Sweden, Finland and the Baltic countries. In the Mediterranean, projected decrease will be less pronounced. Indeed, HPDs will reduce in about 1% in Spain, Atlas and Middle East countries. The low inter-model *SD*

(less than 0.6%; Figure 9b) suggests that models project a similar change, which provides a good certainty for this estimate.

In summer, heavy rainfall is projected to increase in North-Eastern Europe and decrease in the south in agreement with Beniston *et al.* (2007). Atlantic lows are projected to shift their paths northwards during summer (Giorgi and Lionello, 2008). Together with warmer air holding more moisture, precipitation will increase. The highest positive changes in HPDs will take place in North-Eastern Europe and the Scandinavian countries (up to 1.5%; Figure 9c; Table 8) with a medium

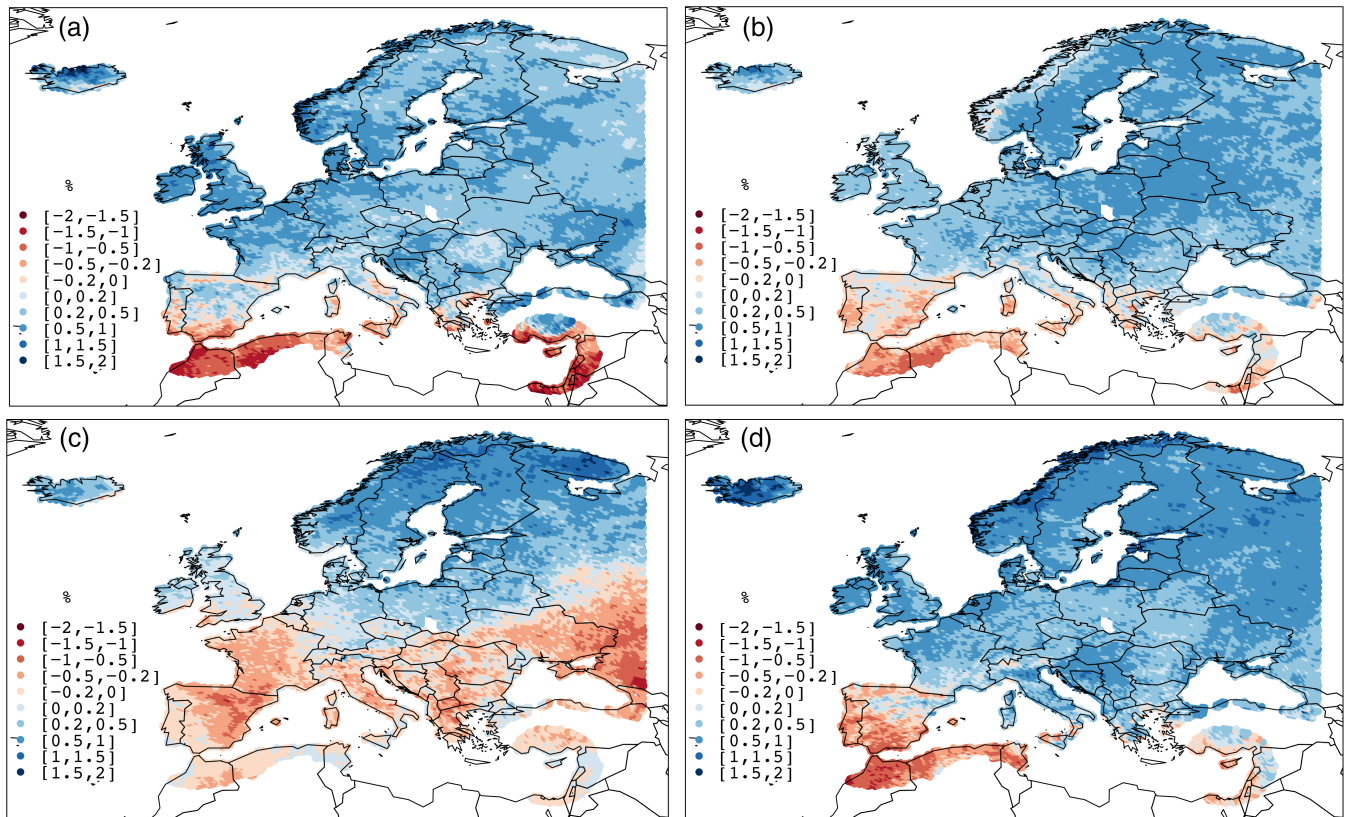


**FIGURE 9** Future change in the percentage of heavy precipitation days in (a) winter, (b) spring, (c) summer and (d) autumn [Colour figure can be viewed at [wileyonlinelibrary.com](http://wileyonlinelibrary.com)]

confidence among models (up to 1% in *SD*; not shown). An interesting rise of this estimate up to 0.5% is expected in United Kingdom, Germany and the Czech Republic despite the pronounced decrease in mean precipitation reported by Christensen and Christensen (2003). On the other hand, results include a possible reduction in heavy summer precipitation in South Eastern Europe and the Mediterranean, in agreement with Jacob *et al.* (2014). This drying might be associated with increased anticyclonic circulations over the region causing a northward shift of the mid-latitude storm track (Giorgi and Lionello, 2008). Central-eastern Europe and Southern Europe will suffer a significant decrease in HPDs of 1.5%. These results present a high confidence given the low inter-model *SD* (less than 0.6%).

Finally, it should be noted that future change of HPDs in autumn will be similar in distribution to that projected for spring but generally stronger, except in some areas of Germany, Poland, Ukraine and Belarus (Figure 9d; Table 8). That is, positive changes between 0.5 and 1.5% in large parts of Europe are foreseen. Models consistently project an increase of HPDs in countries of Central Europe, due to the joint combination of less precipitation days, but larger daily rainfall accumulations (Cardell *et al.*,

2019). These results are consistent across models (not shown). However, HPDs might decrease about 1.5% in the Atlas and Spain owing to the extension of the summery high pressures towards early autumn. These results present a low certainty given the high inter-model *SD* (up to 1.7%).

### 3.2.2 | Heavy precipitation episodes

In Europe, impacts from heavy precipitation are generally due to short-period rainfalls of localized convective activity in summer, and multi-day episodes of persistent large-scale precipitation in winter (Frei *et al.*, 2006). Both kinds of events are projected to become more frequent and intense in large parts of Europe by the end of the century (Ban *et al.*, 2015). In the present work, we consider a heavy precipitation episode (HPE) to be an event of at least two consecutive days ( $d_{th} \geq 2$ ) with daily accumulated precipitation above the observed annual *Precip95* (Table 7). Recall that 95th percentiles are computed by only considering wet days. HPEs have been characterized by their amplitude to determine whether these events will suppose a flood-related risk in the future. Therefore, heavy precipitation amplitude (HPA) is

**TABLE 8** As in Table 3, but for heavy precipitation days (in %)

	Winter			Spring			Summer			Autumn			
	Present	Early	Late	Present	Early	Late	Present	Early	Late	Present	Early	Late	
<b>IC</b>	1.45	<b>1.65</b>	<b>1.75</b>	<b>1.99</b>	<b>1.99</b>	<b>1.99</b>	1.03	<b>1.23</b>	<b>1.38</b>	<b>1.44</b>	1.70	<b>2.06</b>	<b>2.86</b>
±	0.04	0.01	0.02	0.01	0.01	0.01	0.03	0.01	0.01	0.02	0.04	0.02	0.03
<b>WE</b>	1.29	<b>1.41</b>	<b>1.60</b>	<b>1.84</b>	<b>1.98</b>	<b>1.18</b>	1.10	1.09	1.05	1.02	1.80	2.00	<b>2.32</b>
±	0.04	0.02	0.02	0.03	0.02	0.03	0.04	0.04	0.04	0.04	0.05	0.06	0.06
<b>WM</b>	1.69	1.54	1.55	1.35	1.00	<b>0.91</b>	0.38	0.34	<b>0.25</b>	<b>0.17</b>	1.99	<b>1.89</b>	<b>1.68</b>
±	0.08	0.07	0.08	0.06	0.05	0.05	0.03	0.02	0.02	0.01	0.07	0.11	0.11
<b>SC</b>	0.59	<b>0.70</b>	<b>0.85</b>	<b>1.03</b>	<b>0.63</b>	<b>0.97</b>	2.29	<b>2.59</b>	<b>2.75</b>	<b>2.92</b>	1.52	<b>1.82</b>	<b>2.28</b>
±	0.03	0.01	0.01	0.02	0.03	0.02	0.05	0.05	0.05	0.05	0.04	0.03	0.03
<b>CE</b>	0.91	<b>1.02</b>	<b>1.16</b>	<b>1.31</b>	<b>0.97</b>	<b>1.28</b>	1.59	1.64	1.69	1.64	1.54	1.72	<b>1.97</b>
±	0.03	0.02	0.02	0.02	0.04	0.03	0.04	0.05	0.06	0.06	0.05	0.05	0.07
<b>CM</b>	1.40	1.40	1.57	1.46	0.89	0.95	0.64	0.61	<b>0.53</b>	<b>0.47</b>	2.08	2.26	2.32
±	0.06	0.05	0.07	0.06	0.04	0.05	0.03	0.05	0.04	0.03	0.07	0.10	0.14
<b>EE</b>	0.44	<b>0.55</b>	<b>0.72</b>	<b>0.84</b>	0.86	<b>1.22</b>	2.33	2.42	2.36	<b>2.23</b>	1.39	1.65	1.92
±	0.02	0.01	0.02	0.02	0.03	0.04	0.06	0.12	0.13	0.14	0.05	0.06	0.09
<b>EM</b>	2.46	2.44	2.49	2.38	0.75	0.79	0.44	0.44	0.35	<b>0.35</b>	1.39	1.60	<b>1.52</b>
±	0.09	0.09	0.11	0.09	0.04	0.04	0.02	0.03	0.03	0.03	0.06	0.09	0.10
<b>NE</b>	0.21	<b>0.30</b>	<b>0.40</b>	<b>0.54</b>	0.62	<b>0.98</b>	2.76	3.11	<b>3.24</b>	3.26	1.45	<b>1.77</b>	<b>2.18</b>
±	0.01	0.01	0.01	0.01	0.03	0.02	0.06	0.06	0.06	0.07	0.04	0.03	0.03

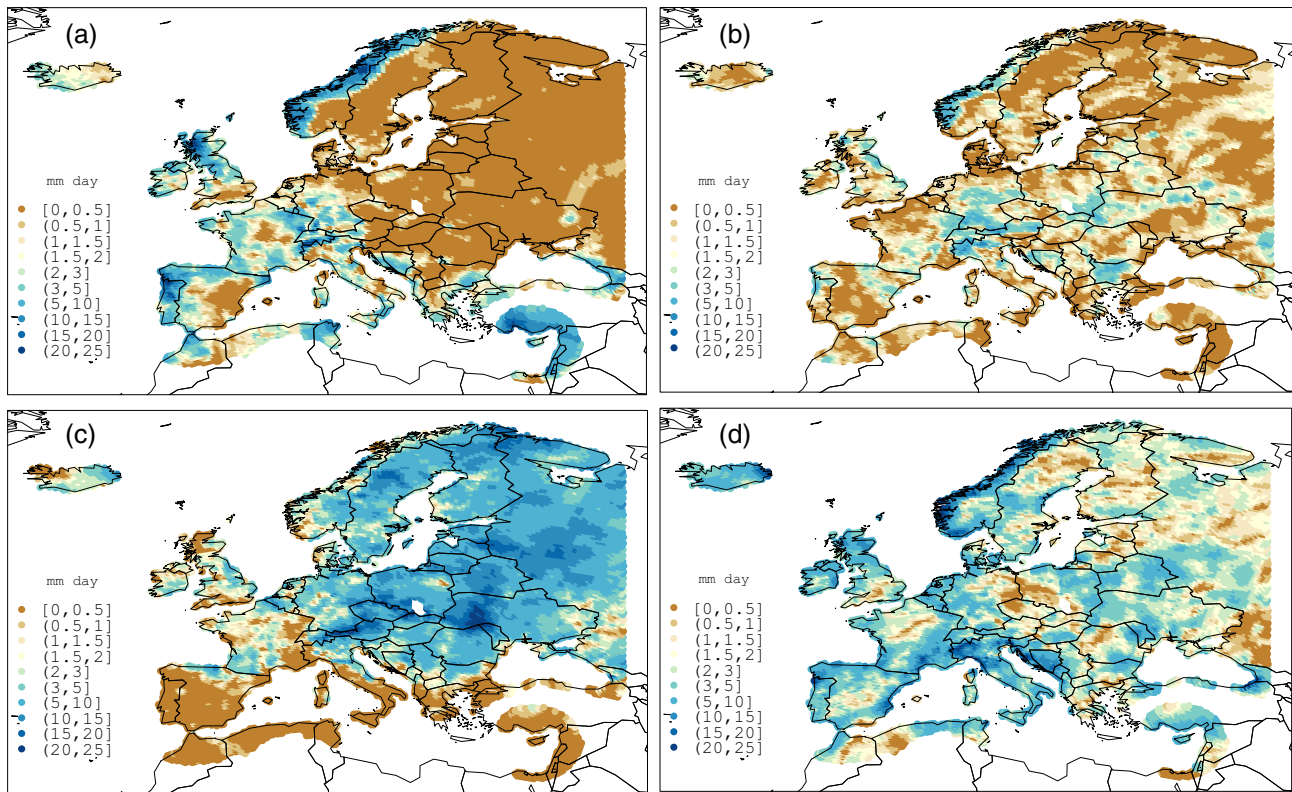


**FIGURE 10** Present observed heavy precipitation amplitude in (a) winter, (b) spring, (c) summer and (d) autumn [Colour figure can be viewed at [wileyonlinelibrary.com](http://wileyonlinelibrary.com)]

defined as the accumulated rainfall stress exceedance for all the days under extreme wet conditions in a given time interval. It is expressed in mm day and is specifically defined as:

$$\text{HPA} = \text{THP} - \text{Precip95} \cdot \text{HPF} \quad (8)$$

Total heavy precipitation (THP) in Equation (8) is defined as the integral of the daily rainfall over the duration of each individual heavy precipitation episode, and accumulated for all HPEs in the time interval. HPF represents the heavy precipitation day frequency (in days).

In the present climate, the accumulated rainfall stress exceedance over Europe responds to a similar spatial pattern to that of HPD (Figure 10; Table 9). We find a remarkable geographical dipole between north and south Europe in winter and summer. HPA is higher (lower) in south-western maritime (North-Eastern) Europe in winter which is between 2–20 (up to 2) mm day. Summer presents a stronger (lower) HPA up to 25 (below 3) mm day in middle and North-Eastern (South-Western) Europe. In spring, HPA is only significant on much delimited regions such as the highlands, Southern Germany, Austria and northern Norway. The accumulated rainfall stress exceedance distributes uniformly throughout the domain in autumn, but is quite pronounced in the

Mediterranean. This higher exceedance is attributed to the leading role of moist convection associated with the presence of relative warm sea surface temperatures, acting as source of high moisture at low levels, combined with the upper-level intrusion of cold air from the north over the Mediterranean.

Projections point out an overall HPA rise across seasons by 2071–2095, except in some limited areas of Spain, Scandinavia, United Kingdom, the Alps and Turkey (Figure 11; Table 9). In winter, the positive signal will be considerable in numerous regions of South Eastern Europe and the Mediterranean (between 3–15 mm day; Figure 11a). However, the projected decrease of the HPDs combined with the HPA rise in Southern Spain and Turkey suggests that heavy precipitation might increasingly concentrate in less but more severe wintry episodes. The vulnerability of the Iberian Peninsula, associated with its transition from more arid to wetter climates to the south and north of its geographical position, respectively, is also present for this estimate. Indeed, northern Spain and Portugal will suffer a significant decrease of 15 mm day with a broad agreement among models. Likewise, HPA will substantially reduce in about 15 mm day in some areas of United Kingdom, the Alps, Nordic countries and Middle East countries. These results present a medium confidence among models (between 3–7 mm day in *SD*; not shown).

**TABLE 9** As in Table 3, but for heavy precipitation amplitude (in mm day)

	Winter			Spring			Summer			Autumn				
	Present	Early	Late	Present	Early	Late	Present	Early	Late	Present	Early	Late		
<b>IC</b>	2.10	<b>2.48</b>	<b>3.23</b>	<b>4.38</b>	<b>1.82</b>	<b>2.44</b>	<b>2.69</b>	<b>3.56</b>	<b>3.78</b>	<b>4.37</b>	6.03	5.18	8.69	<b>11.31</b>
±	5.18	2.63	3.63	4.40	2.94	3.66	3.95	4.56	4.74	5.63	10.63	4.81	9.94	12.58
<b>WE</b>	3.09	2.78	3.80	<b>5.20</b>	2.40	3.24	4.00	5.27	6.22	6.17	4.34	7.26	7.86	<b>9.41</b>
±	7.47	4.00	5.29	6.47	4.25	5.98	7.66	11.39	12.47	11.89	9.16	14.47	17.37	17.38
<b>WM</b>	3.15	4.47	5.30	4.98	1.04	2.82	<b>2.98</b>	<b>1.74</b>	<b>1.33</b>	1.02	4.21	8.03	7.88	7.73
±	8.21	10.34	11.96	11.40	4.00	7.26	7.97	4.78	3.44	2.79	10.61	18.80	20.97	21.14
<b>SC</b>	1.53	1.39	1.46	2.51	0.94	<b>2.60</b>	<b>2.88</b>	9.47	10.46	<b>12.70</b>	3.70	4.22	5.27	<b>6.88</b>
±	3.18	2.09	2.01	3.60	3.93	4.56	4.69	11.94	13.49	15.70	7.80	5.68	7.31	9.17
<b>CE</b>	2.65	2.54	3.82	<b>4.40</b>	3.62	5.35	<b>6.19</b>	8.42	<b>11.87</b>	<b>11.72</b>	5.34	8.81	9.96	11.91
±	6.72	3.98	6.13	6.57	5.80	9.24	10.44	13.17	21.89	21.47	11.35	16.63	22.16	23.95
<b>CM</b>	2.40	4.11	5.49	4.81	<b>2.87</b>	<b>3.61</b>	<b>4.08</b>	3.42	3.32	2.93	4.62	9.79	12.24	12.82
±	7.15	8.90	13.26	12.34	6.29	9.53	10.22	10.32	9.84	8.31	11.15	20.03	31.26	33.12
<b>EE</b>	0.33	0.65	<b>1.15</b>	<b>1.52</b>	<b>2.97</b>	<b>3.86</b>	<b>5.16</b>	7.42	15.40	15.59	3.01	4.94	6.94	<b>8.35</b>
±	1.24	1.33	2.12	3.13	5.14	8.00	10.18	28.38	35.23	41.74	8.05	10.06	16.10	20.35
<b>EM</b>	6.50	6.77	7.46	7.46	<b>3.32</b>	2.51	<b>3.11</b>	<b>2.54</b>	<b>2.07</b>	<b>2.53</b>	3.93	7.19	8.03	8.46
±	13.66	13.27	17.56	17.23	2.70	6.72	7.77	7.21	6.14	7.29	11.38	17.91	21.07	22.76
<b>NE</b>	0.05	<b>0.14</b>	<b>0.14</b>	<b>0.43</b>	1.76	<b>2.11</b>	<b>2.88</b>	9.07	12.37	14.83	2.14	2.61	3.09	<b>4.00</b>
±	0.26	0.42	0.33	1.00	2.91	3.46	4.86	13.88	14.87	22.05	5.37	3.55	3.98	5.08

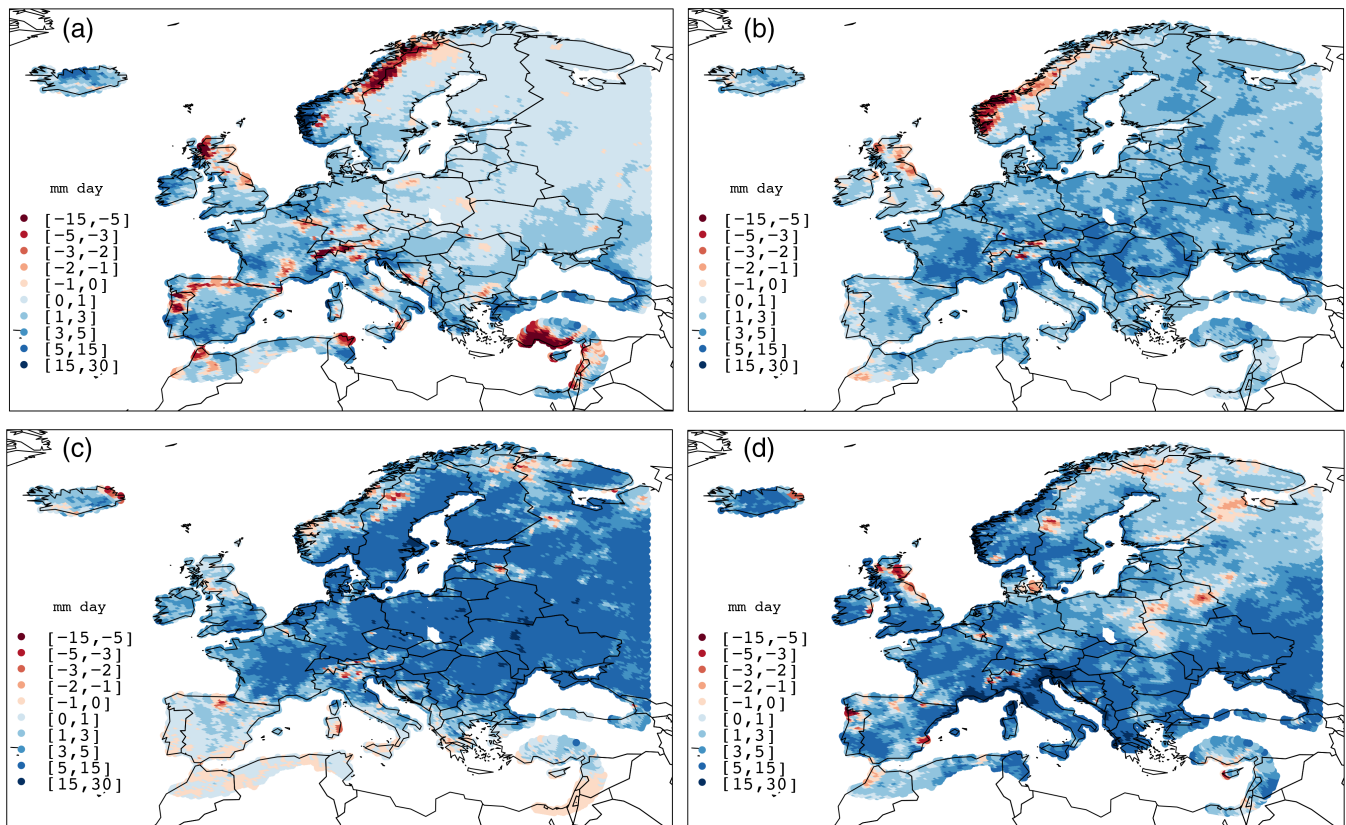


**FIGURE 11** Future change in heavy precipitation amplitude for (a) winter, (b) spring, (c) summer and (d) autumn [Colour figure can be viewed at [wileyonlinelibrary.com](http://wileyonlinelibrary.com)]

Concerning the spring contribution, only west Sweden, and some dispersed areas of United Kingdom and the Alps will experience HPA decreases. Intensification of the heavy precipitation amplitude might be considerable in countries of Western and Central Europe (Figure 11b; Table 9). Results are in agreement with the mean rainfall and HPDs increase projected for these regions (Cardell *et al.*, 2019). For example, a positive signal of HPA up to 15 mm day might be expected in Southern France, northern Italy, Serbia and Hungary, among others. A comparable change for this estimate seems to be projected among models, according to the low values of inter-model *SD* (less than 7 mm day; not shown). Note that the expected changes for the late future period would be significant at 95% level of confidence for most European/Mediterranean regions (Table 9).

While the intensification of HPA is robust across models in winter and spring, increases in middle and north Europe are subject to large uncertainty in summer. HPA might increase up to 15 mm day in these areas (Figure 11c) but with a low agreement among models (above 7 mm day in *SD*; not shown). The expected increase over these regions would be a consequence of the enhancement of atmospheric instability and

convective activity associated with a warmer and more humid lower troposphere. In Southern Europe, models tend to project a slight intensification of HPA; despite important decreases of mean rainfall and rainy days in South Eastern Europe and the Mediterranean as well (Cardell *et al.*, 2019).

In autumn, Southern France and northern Italy could suffer important positive changes of HPA by the late 21st century (up to 30 mm day; Figure 11d). However, the high inter-model *SD* suggests poor confidence in this result (above 15 mm day; not shown). In the Mediterranean, although the frequency of HPDs will decrease, precipitations are expected to be more extreme due to an intensification of the HPA. This change in extreme rainfall regimes would be also associated with more atmospheric instability. Warmer and more humid air at low levels together with fewer upper-air cold air intrusions from the north will produce less but more violent convection in this region. Projections also show considerable HPA increases in other countries of South Eastern Europe and the Mediterranean, where present *Precip95* in annual rainfall amounts are extremely high (above 40 mm). For example, Iberian Peninsula, France, United Kingdom and western coast of Nordic countries

**TABLE 10** As in Table 3, but for number of dry days

	Winter			Spring			Summer			Autumn						
	Present	Early	Mid	Late	Present	Early	Mid	Late	Present	Early	Mid	Late				
<b>IC</b>	32.39	<b>32.80</b>	34.08	33.10	43.95	43.68	45.33	45.60	48.20	49.20	48.04	48.89	37.68	37.64	37.64	<b>37.08</b>
±	7.65	3.87	4.38	3.75	8.07	5.89	5.65	6.01	7.88	6.14	6.13	6.07	6.29	4.69	4.81	5.09
<b>WE</b>	42.90	43.18	44.25	45.27	48.22	48.78	50.61	53.07	54.99	57.44	<b>62.69</b>	<b>67.21</b>	45.38	47.98	50.32	<b>52.25</b>
±	9.69	6.55	6.46	6.93	9.24	8.77	10.16	10.29	7.62	11.33	10.72	9.72	8.42	10.67	11.64	10.59
<b>WM</b>	64.19	67.33	68.52	<b>80.00</b>	67.01	<b>70.60</b>	<b>75.16</b>	<b>78.36</b>	82.76	<b>85.00</b>	<b>86.82</b>	<b>88.76</b>	67.96	71.20	<b>72.94</b>	<b>75.25</b>
±	9.90	12.43	12.23	10.55	7.21	13.64	12.16	11.59	4.21	7.11	5.66	3.72	6.59	14.49	14.77	13.88
<b>SC</b>	45.11	<b>46.82</b>	<b>47.11</b>	<b>46.79</b>	56.94	58.08	57.08	56.74	48.77	48.22	48.50	49.13	46.16	47.32	48.55	49.54
±	8.55	4.85	4.94	4.91	6.62	9.77	9.11	9.43	8.74	10.98	10.91	10.01	8.02	7.95	8.51	8.15
<b>CE</b>	51.82	51.91	52.52	53.19	52.84	52.94	53.98	55.32	53.36	55.37	57.86	<b>62.24</b>	53.20	55.07	57.24	59.39
±	8.65	7.38	7.52	7.73	7.22	10.33	10.94	11.42	7.05	12.94	12.75	12.36	8.35	12.44	13.82	13.22
<b>CM</b>	60.41	62.32	63.54	<b>66.34</b>	65.50	69.03	<b>73.02</b>	<b>76.58</b>	78.18	<b>81.39</b>	<b>83.02</b>	<b>84.87</b>	65.83	67.52	68.49	<b>71.27</b>
±	8.43	10.17	10.90	10.34	6.08	11.41	12.07	10.42	5.30	11.89	10.52	8.22	6.29	13.36	15.60	15.02
<b>EE</b>	53.56	54.86	55.71	<b>56.03</b>	59.93	60.69	60.92	61.29	58.66	60.62	61.92	<b>64.55</b>	59.99	61.58	62.53	64.35
±	7.16	7.18	7.53	7.55	6.61	12.78	13.66	13.64	6.91	18.56	18.50	18.99	7.57	13.66	15.11	15.39
<b>EM</b>	56.90	58.56	<b>60.49</b>	<b>62.82</b>	65.97	68.50	71.17	<b>73.37</b>	80.15	81.85	83.29	<b>84.03</b>	72.00	<b>74.09</b>	<b>75.26</b>	<b>76.50</b>
±	7.63	11.72	13.20	12.21	6.79	12.81	12.87	11.62	4.39	9.12	7.92	7.13	5.48	13.75	14.71	14.16
<b>NE</b>	39.31	<b>41.45</b>	<b>41.27</b>	<b>41.04</b>	55.31	57.24	56.42	56.63	49.68	48.91	48.59	50.19	43.24	43.80	45.39	<b>46.56</b>
±	8.11	3.76	4.08	4.52	6.12	9.99	9.64	10.30	8.69	11.77	11.47	11.29	8.46	8.32	8.37	8.39

will experience an intensification up to 15 mm day with a general agreement among models.

### 3.2.3 | Dry days

Reduced precipitation is a facet of climate change that can particularly affect societies and ecosystems in some regions of Europe. Among other sectors, tourism and agriculture may be potentially influenced by changes in the frequency of days without rainfall. In the present work, a dry day has been defined as an event in which daily precipitation values are below 0.1 mm (Table 7). The present section analyses future changes in the frequency of dry days and have been expressed as percentage shifts relative to the total amount of dry days in the present.

Projections point out an overall increase in the annual number of dry days over Europe, except in some areas of Scandinavia. Dry day increases will be particularly pronounced around the Mediterranean Sea in line with Polade *et al.* (2014). Recall that most of Europe will be exposed to an intensification of HPA. However, the Mediterranean might be dominated by an increase in dry days rather than by changes in precipitation owing to a

northward deflection of the Atlantic storm track (Giorgi and Lionello, 2008). Increased anticyclonic conditions over the Mediterranean may generally lead to higher atmospheric stability and less favourable conditions to storm generation. According to our results, dry days will also intensify in south-western maritime Europe. The Iberian Peninsula and the Balkans feature the largest increases in the number of dry days (above 24%; not shown). Likewise, France and United Kingdom will suffer a substantial increase (above 12%), with a good confidence among models (less than 10% in *SD*; not shown). It must be noted that in these regions approximately 230 days per year are considered dry in the present.

The assessment of dry days across seasons shows a significant increase in dryness by 2071–2095, except in some areas of Scandinavia, north Germany and the Baltic countries during spring and summer. According to the Kolmogorov–Smirnov test, the expected increase would be statistically significant in the Mediterranean regions throughout seasons (Table 10). Recall that in the present, between 20–52 days are considered dry in Central and Northern Europe, while in Southern countries the number of dry days varies between 52–92 depending on the season (Figure 12). Indeed, the largest increases of dry

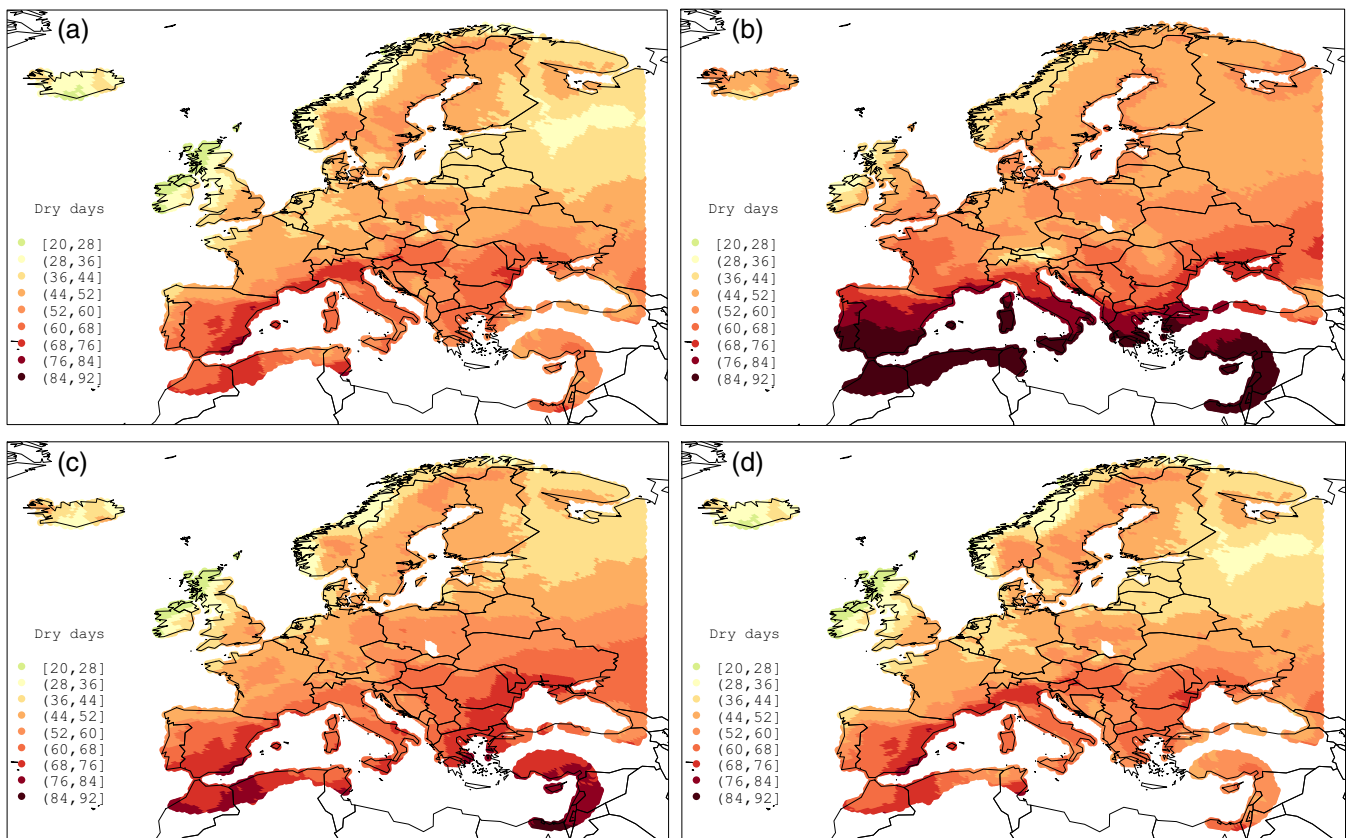


**FIGURE 12** Present observed number of dry days in (a) winter, (b) spring, (c) summer and (d) autumn [Colour figure can be viewed at [wileyonlinelibrary.com](http://wileyonlinelibrary.com)]

days will be expected in south-western maritime Europe in summer and spring by 2071–2095 (above 20%), while reducing by 9% in some areas of Northern Europe and Baltic countries (Figure 13). Precipitation deficit during spring would play an important role in enhancing summery heat wave episodes over the Mediterranean owing to the associated depletion of soil moisture and the subsequent reduced cooling effect via latent heat exchange (Fischer *et al.*, 2007). In winter and autumn, increases in the number of dry days are not so dramatic over the former regions, while reducing in some scattered areas of Scandinavia. Positive changes are quite consistent across models, while decreases present a low certainty according to the high *SD* (not shown).

### 3.2.4 | Droughts

Once changes in the frequency of dry days have been assessed, a major concern arises in how droughts are expected to change under human-induced climate change. That is, whether individual future dry days could reorganize to give place to more extended consecutive periods without rain, resulting in longer droughts. To

answer this question, we first define a dry spell as a period of at least three consecutive dry days. The 95th percentile of the length of all identified dry spells in the present period is used as the threshold to define a drought: any consecutive period of dry days longer than this threshold is considered a drought (Table 7).

Hence, it is possible to encompass the distinct impacts of droughts depending on the regional climatology. Impacts differ among the different European climates. For instance, the Mediterranean faces inherent long periods of summer droughts. Ecosystems and populations are well adapted to these periods. In temperate climates, less persistent droughts can result in substantial impacts on population and environment. The present occurrence of persistent droughts is considerable across Europe. Nearly two droughts per year longer than 8 days are found in countries of Central Europe such as Germany, Austria and Czech Republic (Figure 14a,b; Table 11). Some scattered areas of Scandinavia present more than two droughts per year lasting from 8 to 18 consecutive days. In contrast, the frequency of droughts is lower in the Mediterranean, owing to their extremely extended length. As an example, Southern Iberian Peninsula presents approximately one drought per year with a duration up to 100 consecutive days.

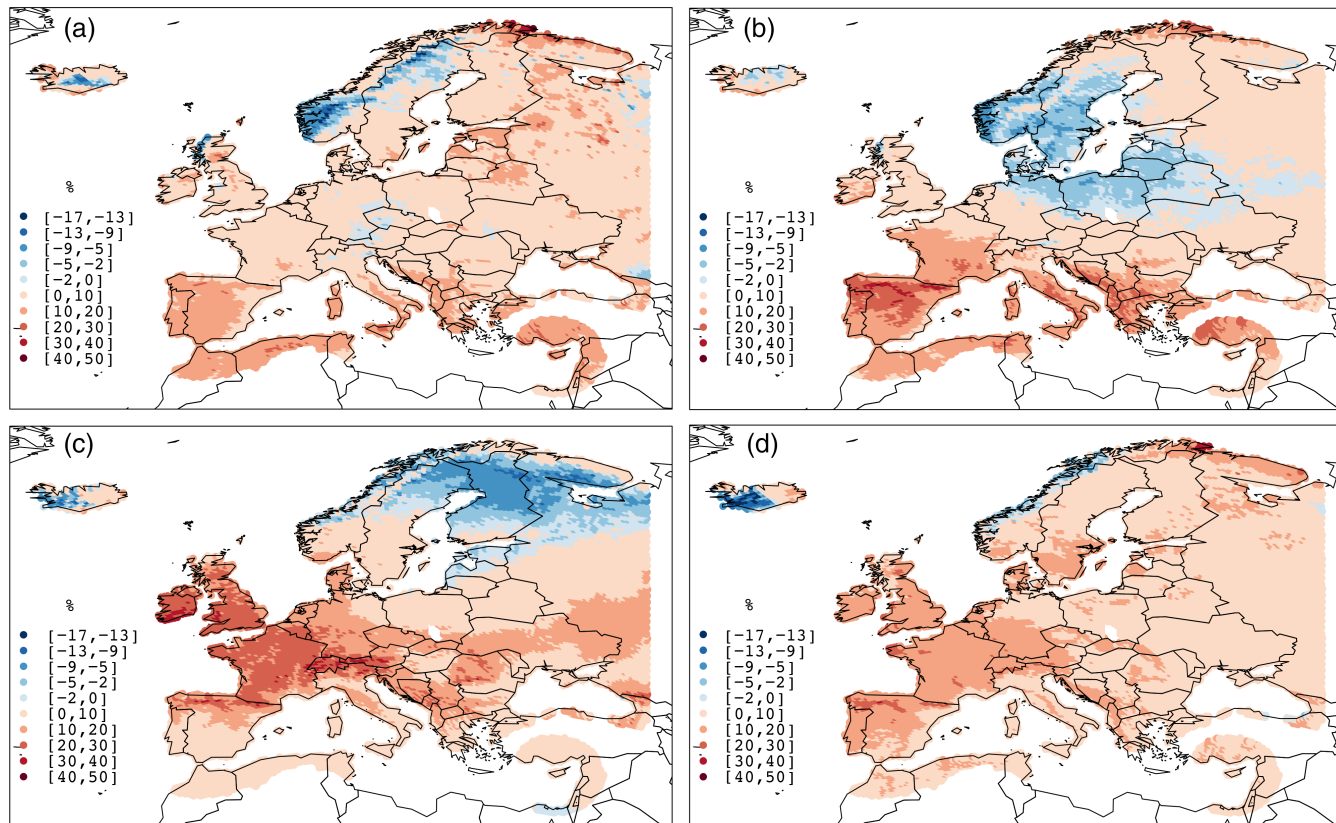


**FIGURE 13** Future percentage change in the number of dry days for (a) winter, (b) spring, (c) summer and (d) autumn [Colour figure can be viewed at [wileyonlinelibrary.com](http://wileyonlinelibrary.com)]

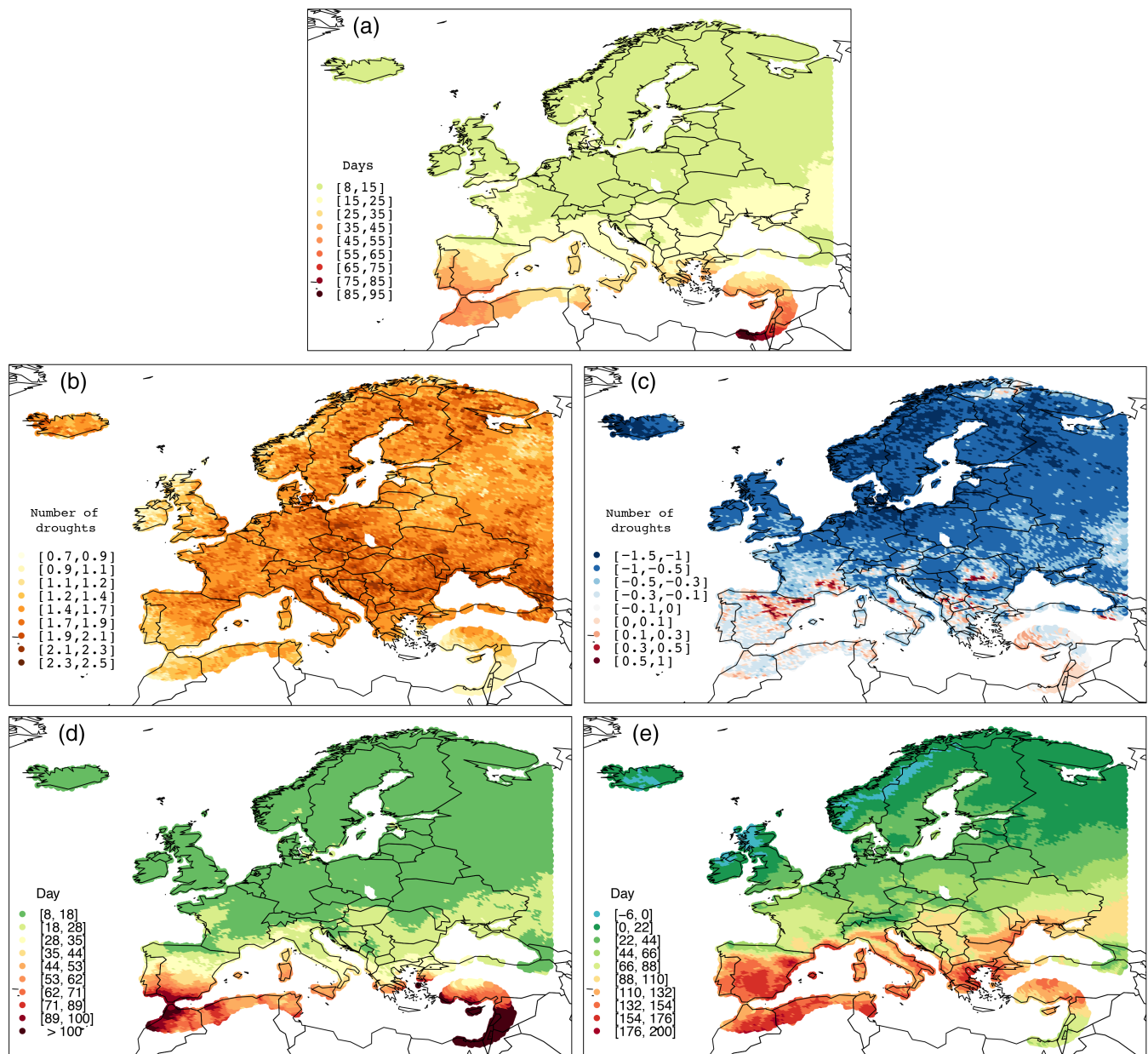


**FIGURE 14** (a) Present observed 95th percentile of dry spell lengths (1981–2005) used to define a drought; (b) present observed number of droughts and (c) future change in the number of droughts. Also shown: (d) present observed mean drought length and (e) future change of this length [Colour figure can be viewed at [wileyonlinelibrary.com](http://wileyonlinelibrary.com)]

Future changes in the annual pattern of droughts indicate an increase in occurrence and severity over the Mediterranean by 2071–2095 in line with previous studies (Dubrovský *et al.*, 2014; Hertig and Trambly, 2017). According to our definition, patterns of the annual drought occurrence are quite different depending on the region, showing positive or negative changes even in the same country. For example, North-Eastern Spain, south-eastern France and some areas of Italy and Balkans will present one drought more per year with a length up to 28 additional days (Figure 14c,d). In contrast, number of droughts will likely reduce in the

remaining parts of these countries, but their duration will notably increase more than 3 months. These results present a high inter-model variability. Finally, models consistently project that the number of droughts will also reduce in Central and Northern Europe (between  $-0.5$  and  $-1.5$ ), despite the large increase in length (up to 66 days). It is important to note that the estimated decrease in the number of droughts would be significant for the early future (Table 11). Conversely, all the projected increases in drought length would be notable at 95% level of significance over all the continent from early future.

**TABLE 11** As in Table 3, but for the number of annual droughts and drought length (in days)

	Number Present				Length Present			
	Early	Mid	Late		Early	Mid	Late	
<b>IC</b>	1.56	<b>0.47</b>	<b>0.49</b>	<b>0.54</b>	10.47	12.99	12.02	13.81
±	1.34	0.49	0.51	0.49	6.50	22.14	20.11	20.38
<b>WE</b>	1.50	<b>0.61</b>	<b>0.78</b>	<b>0.98</b>	15.20	<b>41.84</b>	<b>49.79</b>	<b>58.84</b>
±	1.06	0.52	0.49	0.45	7.41	49.66	50.72	51.41
<b>WM</b>	1.44	<b>1.13</b>	1.27	1.39	52.51	<b>158.83</b>	<b>172.72</b>	<b>190.16</b>
±	0.81	0.28	0.24	0.25	21.77	84.14	81.31	80.35
<b>SC</b>	1.59	<b>0.63</b>	<b>0.65</b>	<b>0.70</b>	13.92	<b>30.94</b>	<b>30.10</b>	<b>30.96</b>
±	1.15	0.51	0.50	0.49	7.19	43.48	42.14	42.55
<b>CE</b>	1.72	<b>0.78</b>	<b>0.90</b>	<b>1.11</b>	16.31	<b>51.14</b>	<b>57.03</b>	<b>64.88</b>
±	1.18	0.56	0.57	0.51	7.49	63.57	64.87	66.33
<b>CM</b>	1.65	<b>1.24</b>	1.33	1.49	36.56	<b>130.26</b>	<b>144.53</b>	<b>159.10</b>
±	0.97	0.33	0.30	0.30	16.12	81.52	82.30	82.08
<b>EE</b>	1.74	<b>0.95</b>	<b>1.00</b>	1.17	17.41	<b>72.58</b>	<b>78.52</b>	<b>85.37</b>
±	1.24	0.54	0.55	0.50	8.22	77.10	78.87	79.46
<b>EM</b>	1.42	<b>1.14</b>	<b>1.21</b>	1.30	73.87	<b>151.85</b>	<b>164.65</b>	<b>173.53</b>
±	0.72	0.28	0.25	0.24	21.18	74.79	75.36	75.68
<b>NE</b>	1.52	<b>0.61</b>	<b>0.62</b>	<b>0.73</b>	12.78	<b>28.75</b>	<b>28.10</b>	<b>30.95</b>
±	1.09	0.49	0.49	0.49	6.95	39.39	38.93	41.45

#### 4 | CONCLUSIONS AND FURTHER REMARKS

This paper analyses human-induced future shifts in European temperature and precipitation extremes by using a combination of dynamical and statistical procedures. Future changes have been discussed by means of several diagnostics applied to daily observed and projected temperatures and accumulated precipitation. A Q–Q adjustment method was applied to the simulated meteorological variables to correct possible biases in the RCMs representations of local climates. The design of a set of novel climatic indices permits to properly encompass extreme regimes. The main conclusions of this study are:

- Warm extremes will dramatically increase in all seasons over the entire Europe. Summer will be the most affected season, particularly in the southern countries. Northern regions project the largest increase in the number of warm days during spring. Conversely, autumn would entail the biggest increments in the southern areas of the continent.
- The Mediterranean countries might be especially vulnerable due to the important increase in summery heat wave amplitude. In the shoulder seasons, positive changes in this estimate will resemble the

same geographical pattern than the number of warm days.

- The presence of cold nights will likely reduce across Europe consistently with the diminution in warm day frequency. The most affected regions might be Scandinavia and Northern-Eastern Europe.
- Cold spells are coherently projected to be less frequent and severe across Europe with a notably decrease in cold spell amplitude over Northern Europe.
- Heavy precipitation days are expected to increase in Central and Northern Europe across seasons, while decreasing in some regions of the Mediterranean. Interestingly enough, a rise in summery heavy precipitation days is projected in United Kingdom, Germany and Czech republic, despite the significant decrease of mean precipitation. Summery and autumnal growths will be associated with less rainy days, but with larger rainfall amounts.
- Heavy precipitation amplitude will feature an overall rise across seasons. Wintery increments will be more significant in Southern Europe, while in summer are predicted to be larger in central and northern regions. Western and Central Mediterranean would suffer the more severe intensification in the hydrological cycle.
- Despite the projected increment in heavy precipitation days and amplitude, future dry periods are expected to exacerbate in Europe. Only some northern regions and

the Baltic countries might exhibit an increase in the number of rainy days.

- Shifts in drought pattern strengthen the projected dryness over the Mediterranean owing to the occurrence of more persistent droughts. In general, the number of droughts will reduce over Europe as consequence of projected increases in length.

The information here provided can be useful for future climate research and impact assessment. Moreover, policy makers and stakeholders could establish new adaptation procedures to face with the challenges imposed by changes in the extreme weather regimes. In view of the important projected increases in heat wave amplitude, not only in summer but also in the shoulder seasons, we plan as future work to explore heat wave impacts on human health across the European and Mediterranean countries by considering thermal stress indices derived from energy budget models of the human body.

## ACKNOWLEDGEMENTS

This research is framed within the CGL2014-52199-R (EXTREMO) and CGL2017-82868-R (COASTEPS) projects, both of them funded by the Spanish “Ministerio de Economía, Industria y Competitividad” and partially supported with FEDER funds. The first author was also supported by the FPI-CAIB (FPI/1931/2016) grant from the Conselleria d’Innovació, Recerca i Turisme del Govern de les Illes Balears and the Fons Social Europeu. The authors acknowledge the EURO-CORDEX project, sponsored by the World Climate Research Program (WRCP). The E-OBS data set from the EU-FP6 project and data providers in the ECA and D project (eca.knmi.nl) are also acknowledged.

## ORCID

Maria F. Cardell  <https://orcid.org/0000-0002-8856-8666>

## REFERENCES

- Alexander, L., Zhang, X., Peterson, T., Caesar, J., Gleason, B., Klein Tank, A., Haylock, M., Collins, D., Trewin, B., Rahimzadeh, F., et al. (2006) Global observed changes in daily climate extremes of temperature and precipitation. *Journal of Geophysical Research: Atmospheres*, 111, D05109. <https://doi.org/10.1029/2005JD006290>.
- Amengual, A., Homar Santaner, V., Romero, R., Brooks, H., Ramis, C., Gordaliza, M. and Alonso, S. (2014) Projections of heat waves with high impact on human health in Europe. *Global and Planetary Change*, 119, 71–84. <https://doi.org/10.1016/j.gloplacha.2014.05.006>.
- Ban, N., Schmidli, J. and Schär, C. (2015) Heavy precipitation in a changing climate: does short-term summer precipitation increase faster? *Geophysical Research Letters*, 42(4), 1165–1172. <https://doi.org/10.1002/2014GL025888>.
- Barcikowska, M., Kapnick, S., Krishnamurty, L., Russo, S., Cherchi, A. and Folland, C. (2019) Changes in the future summer mediterranean climate: contribution of teleconnections and local factors. *Earth System Dynamics Discussions*, 1–43. <https://doi.org/10.5194/esd-2018-85>.
- Beniston, M. (2004) The 2003 heat wave in Europe: a shape of things to come? An analysis based on Swiss climatological data and model simulations. *Geophysical Research Letters*, 31 (L02202). <https://doi.org/10.1029/2003GL018857>.
- Beniston, M. and Stephenson, D.B. (2004) Extreme climatic events and their evolution under changing climatic conditions. *Global and Planetary Change*, 44, 1–9. <https://doi.org/10.1016/j.gloplacha.2004.06.001>.
- Beniston, M., Stephenson, D.B., Christensen, O.B., Ferro, C.A., Frei, C., Goyette, S., Halsnaes, K., Holt, T., Jylhä, K., Koffi, B., et al. (2007) Future extreme events in European climate: an exploration of regional climate model projections. *Climatic Change*, 81 (1), 71–95. <https://doi.org/10.1007/s10584-006-9226-z>.
- Cardell, M., Romero, R., Amengual, A., Homar, V. and Ramis, C. (2019) A quantile-quantile adjustment of the Euro-cordex projections for temperatures and precipitation. *International Journal of Climatology*, 39(6), 2901–2918. <https://doi.org/10.1002/joc.5991>.
- Casanueva, A., Kotlarski, S., Herrera, S., Fernández, J., Gutiérrez, J. M., Boberg, F., Colette, A., Christensen, O.B., Goergen, K., Jacob, D., Keuler, K., Nikulin, G., Teichmann, C. and Vautard, R. (2016) Daily precipitation statistics in a Euro-cordex rcm ensemble: added value of raw and bias-corrected high-resolution simulations. *Climate Dynamics*, 47(3–4), 719–737. <https://doi.org/10.1007/s00382-015-2865-x>.
- Casanueva, A., Rodríguez-Puebla, C., Frías, M.D. and González-Reviriego, N. (2014) Variability of extreme precipitation over Europe and its relationships with teleconnection patterns. *Hydrology and Earth System Sciences*, 18(2), 709–725. <https://doi.org/10.5194/hess-18-709-2014>.
- Christensen, J.H. and Christensen, O.B. (2003) Climate modelling: severe summertime flooding in Europe. *Nature*, 421(6925), 805–806. <https://doi.org/10.1038/421805a>.
- Christensen, J.H. and Christensen, O.B. (2007) A summary of the prudence model projections of changes in European climate by the end of this century. *Climatic Change*, 81(1), 7–30. <https://doi.org/10.1007/s10584-006-9210-7>.
- de Vries, H., Haarsma, R.J. and Hazeleger, W. (2012) Western European cold spells in current and future climate. *Geophysical Research Letters*, 39(L04706). <https://doi.org/10.1029/2011GL050665>.
- Donat, M., Alexander, L., Yang, H., Durre, I., Vose, R., Dunn, R., Willett, K., Aguilar, E., Brunet, M., Caesar, J., et al. (2013) Updated analyses of temperature and precipitation extreme indices since the beginning of the twentieth century: the hadex2 dataset. *Journal of Geophysical Research: Atmospheres*, 118(5), 2098–2118. <https://doi.org/10.1002/jgrd.50150>.
- Dosio, A. (2016) Projections of climate change indices of temperature and precipitation from an ensemble of bias-adjusted high-resolution Euro-cordex regional climate models. *Journal of Geophysical Research: Atmospheres*, 121(10), 5488–5511. <https://doi.org/10.1002/2015JD024411>.
- Dubrovský, M., Hayes, M., Duce, P., Trnka, M., Svoboda, M. and Zara, P. (2014) Multi-gcm projections of future drought and

- climate variability indicators for the mediterranean region. *Regional Environmental Change*, 14(5), 1907–1919. <https://doi.org/10.1007/s10113-013-0562-z>.
- Field, C., Barros, V., Dokken, D., Mach, K., Mastrandrea, M.D., Bilir, T.E., Chatterjee, M., Ebi, K.L., Estrada, Y.O., Genova, R. C., Girma, B., Kissel, E.S., Levy, A.N., MacCracken, S., Mastrandrea, P.R. and White, L.L. (Eds.). (2014) *Climate Change 2014: Impacts, Adaptation, and Vulnerability. Part A: Global and Sectoral Aspects. Contribution of Working Group II to the Fifth Assessment Report of the Intergovernmental Panel on Climate Change, Chapter: IPCC, 2014: Summary for Policymakers*. Cambridge, UK, and New York, NY, USA: Cambridge University Press, pp. 1–32.
- Field, C.B., Barros, V., Stocker, T.F., Dahe, Q., Dokken, D.J., Ebi, K. L., Mastrandrea, M.D., Mach, K.J., Plattner, G.-K., Allen, S.K., Tignor, M. and Midgley, P.M. (2012) *Managing the Risks of Extreme Events and Disasters to Advance Climate Change Adaptation: Special Report of the Intergovernmental Panel on Climate Change*. Cambridge, UK and New York, NY, USA: Cambridge University Press, p. 582.
- Fischer, E.M. and Schär, C. (2009) Future changes in daily summer temperature variability: driving processes and role for temperature extremes. *Climate Dynamics*, 33(7–8), 917–935. <https://doi.org/10.1007/s00382-008-0473-8>.
- Fischer, E.M. and Schär, C. (2010) Consistent geographical patterns of changes in high-impact European heatwaves. *Nature Geoscience*, 3(6), 398–403. <https://doi.org/10.1038/ngeo866>.
- Fischer, E.M., Seneviratne, S.I., Lüthi, D. and Schär, C. (2007) Contribution of land-atmosphere coupling to recent European summer heat waves. *Geophysical Research Letters*, 34, L06707. <https://doi.org/10.1029/2006GL029068>.
- Fonseca, D., Carvalho, M., Marta-Almeida, M., Melo-Gonçalves, P. and Rocha, A. (2016) Recent trends of extreme temperature indices for the Iberian Peninsula. *Physics and Chemistry of the Earth, Parts A/B/C*, 94, 66–76. <https://doi.org/10.1016/j.pce.2015.12.005>.
- Frei, C., Schöll, R., Fukutome, S., Schmidli, J. and Vidale, P.L. (2006) Future change of precipitation extremes in Europe: Intercomparison of scenarios from regional climate models. *Journal of Geophysical Research: Atmospheres*, 111(D06105). <https://doi.org/10.1029/2005JD005965>.
- Frich, P., Alexander, L., Della-Marta, P., Gleason, B., Haylock, M., Amg Klein, T. and TC, P. (2002) Observed coherent changes in climatic extremes during 2nd half of the 20th century. *Climate Research*, 19, 193–212. <https://doi.org/10.3354/cr019193>.
- Giannakopoulos, C., Le Sager, P., Bindi, M., Moriondo, M., Kostopoulou, E. and Goodess, C. (2009) Climatic changes and associated impacts in the mediterranean resulting from a 2 c global warming. *Global and Planetary Change*, 68(3), 209–224. <https://doi.org/10.1016/j.gloplacha.2009.06.001>.
- Giorgi, F., Jones, C., Asrar, G.R., et al. (2009) Addressing climate information needs at the regional level: the cordex framework. *World Meteorological Organization (WMO) Bulletin*, 58(3), 175.
- Giorgi, F. and Lionello, P. (2008) Climate change projections for the Mediterranean region. *Global and Planetary Change*, 63(2), 90–104. <https://doi.org/10.1016/j.gloplacha.2007.09.005>.
- Giorgi, F. and Mearns, L.O. (1999) Introduction to special section: regional climate modeling revisited. *Journal of Geophysical Research: Atmospheres*, 104(D6), 6335–6352. <https://doi.org/10.1029/98JD02072>.
- Gobiet, A., Kotlarski, S., Beniston, M., Heinrich, G., Rajczak, J. and Stoffel, M. (2014) 21st century climate change in the European Alps—a review. *Science of the Total Environment*, 493, 1138–1151. <https://doi.org/10.1016/j.scitotenv.2013.07.050>.
- Goodess, C., Anagnostopoulou, C., Bárdossy, A., Frei, C., Harpham, C., Haylock, M. R., Hundecha, Y., Maheras, P., Ribalaygua, J., Schmidli, J., Schmith, T., Tolika, K., Tomozeiu, R., and Wilby, R. (2012). An intercomparison of statistical downscaling methods for Europe and European regions – assessing their performance with respect to extreme temperature and precipitation events. 11. Norwich: Climatic Research Unit Research Publication (CRURP), University of East Anglia.
- Grumm, R.H. (2011) The central European and Russian heat event of July–August 2010. *Bulletin of the American Meteorological Society*, 92(10), 1285–1296. <https://doi.org/10.1175/2011BAMS3174.1>.
- Guo, Y., Punnasiri, K. and Tong, S. (2012) Effects of temperature on mortality in Chiang Mai city, Thailand: a time series study. *Environmental Health*, 11(1), 36. <https://doi.org/10.1186/1476-069X-11-36>.
- Haylock, M., Hofstra, N., Klein Tank, A., Klok, E., Jones, P. and New, M. (2008) A european daily high-resolution gridded data set of surface temperature and precipitation for 1950–2006. *Journal of Geophysical Research: Atmospheres*, 113(D20). <https://doi.org/10.1029/2008JD010201>.
- Hertig, E. and Trambly, Y. (2017) Regional downscaling of mediterranean droughts under past and future climatic conditions. *Global and Planetary Change*, 151, 36–48. <https://doi.org/10.1016/j.gloplacha.2016.10.015>.
- Hirschi, M., Seneviratne, S.I., Alexandrov, V., Boberg, F., Boroneant, C., Christensen, O.B., Formayer, H., Orłowsky, B. and Stepanek, P. (2011) Observational evidence for soil-moisture impact on hot extremes in southeastern europe. *Nature Geoscience*, 4(1), 17–21. <https://doi.org/10.1038/ngeo1032>.
- Jacob, D., Petersen, J., Eggert, B., Alias, A., Christensen, O.B., Bouwer, L.M., Braun, A., Colette, A., Déqué, M., Georgievski, G., Georgopoulou, E., Gobiet, A., Menut, L., Nikulin, G., Haensler, A., Hempelmann, N., Jones, C., Keuler, K., Kovats, S., Kröner, N., Kotlarski, S., Kriegsmann, A., Martin, E., van Meijgaard, E., Moseley, C., Pfeifer, S., Preuschmann, S., Radermacher, C., Radtke, K., Rechid, D., Rounsevell, M., Samuelsson, P., Somot, S., Soussana, J.F., Teichmann, C., Valentini, R., Vautard, R., Weber, B. and Yiou, P. (2014) Euro-cordex: new high-resolution climate change projections for European Impact Research. *Regional Environmental Change*, 14(2), 563–578. <https://doi.org/10.1007/s10113-013-0499-2>.
- James, P., Stohl, A., Spichtinger, N., Eckhardt, S. and Forster, C. (2004) Climatological aspects of the extreme European rainfall of August 2002 and a trajectory method for estimating the associated evaporative source regions. *Natural Hazards and Earth System Science, Copernicus Publications on behalf of the European Geosciences Union*, 4(5/6), 733–746.
- Jones, R., Murphy, J., Hassell, D. and Taylor, R. (2001) *Ensemble Mean Changes in a Simulation of the European Climate of 2071–2100 Using the New Hadley Centre Regional Modelling System HadAM3H*. Hadley Centre Report. Bracknell, UK: Hadley Centre, Met Office.

- Kendon, E.J., Roberts, N.M., Fowler, H.J., Roberts, M.J., Chan, S.C. and Senior, C.A. (2014) Heavier summer downpours with climate change revealed by weather forecast resolution model. *Nature Climate Change*, 4(7), 570–576. <https://doi.org/10.1038/NCLIMATE2258>.
- Kharin, V.V. and Zwiers, F.W. (2000) Changes in the extremes in an ensemble of transient climate simulations with a coupled atmosphere–ocean GCM. *Journal of Climate*, 13(21), 3760–3788. [https://doi.org/10.1175/1520-0442\(2000\)013<3760:CITEIA>2.0.CO;2](https://doi.org/10.1175/1520-0442(2000)013<3760:CITEIA>2.0.CO;2).
- Kjellström, E. (2004) Recent and future signatures of climate change in Europe. *Ambio: A Journal of the Human Environment*, 33(4), 193–199. <https://doi.org/10.1579/0044-7447-33.4.193>.
- Kjellström, E., Bärring, L., Jacob, D., Jones, R., Lenderink, G. and Schär, C. (2007) Modelling daily temperature extremes: recent climate and future changes over Europe. *Climatic Change*, 81(1), 249–265. <https://doi.org/10.1007/s10584-006-9220-5>.
- Klein Tank, A. and Können, G. (2003) Trends in indices of daily temperature and precipitation extremes in Europe, 1946–99. *Journal of Climate*, 16(22), 3665–3680. [https://doi.org/10.1175/1520-0442\(2003\)016<3665:TIIODT>2.0.CO;2](https://doi.org/10.1175/1520-0442(2003)016<3665:TIIODT>2.0.CO;2).
- Klein Tank, A. M. G., Zwiers, F. W., and Zhang, X. (2009). *Guidelines on Analysis of Extremes in a Changing Climate in Support of Informed Decisions for Adaptation*. Climate data and monitoring WCDMP-No. 72, WMO-TD No. 1500, p. 56.
- Meehl, G., Tebaldi, C. and Nychka, D. (2004) Changes in frost days in simulations of twentyfirst century climate. *Climate Dynamics*, 23(5), 495–511. <https://doi.org/10.1007/s00382-004-0442-9>.
- Meehl, G.A. and Tebaldi, C. (2004) More intense, more frequent, and longer lasting heat waves in the 21st century. *Science*, 305(5686), 994–997. <https://doi.org/10.1126/science.1098704>.
- Muchan, K., Lewis, M., Hannaford, J. and Parry, S. (2015) The winter storms of 2013/2014 in the UK: hydrological responses and impacts. *Weather*, 70(2), 55–61. <https://doi.org/10.1002/wea.2469>.
- Nikulin, G., Kjellström, E., Hansson, U., Strandberg, G. and ULLERSTIG, A. (2011) Evaluation and future projections of temperature, precipitation and wind extremes over Europe in an ensemble of regional climate simulations. *Tellus A*, 63, 41–55. <https://doi.org/10.1111/j.1600-0870.2010.00466.x>.
- Peings, Y., Cattiaux, J. and Douville, H. (2013) Evaluation and response of winter cold spells over Western Europe in CMIP5 models. *Climate Dynamics*, 41(11–12), 3025–3037. <https://doi.org/10.1007/s00382-012-1565-z>.
- Perkins, S.E. and Alexander, L.V. (2013) On the measurement of heat waves. *Journal of Climate*, 26(13), 4500–4517. <https://doi.org/10.1175/JCLI-D-12-00383.1>.
- Perkins, S.E., Pitman, A.J., Holbrook, N.J., & McAneney, J. (2007). Evaluation of the AR4 Climate Models' Simulated Daily Maximum Temperature, Minimum Temperature, and Precipitation over Australia Using Probability Density Functions. *Journal of Climate*, 20(17), 4356–4376. <https://doi.org/10.1175/jcli4253.1>
- Polade, S.D., Pierce, D.W., Cayan, D.R., Gershunov, A. and Dettinger, M.D. (2014) The key role of dry days in changing regional climate and precipitation regimes. *Scientific Reports*, 4, 4364. <https://doi.org/10.1038/srep04364>.
- Poumadere, M., Mays, C., Le Mer, S. and Blong, R. (2005) The 2003 heat wave in France: dangerous climate change here and now. *Risk Analysis: An International Journal*, 25(6), 1483–1494. <https://doi.org/10.1111/j.1539-6924.2005.00694.x>.
- Rajczak, J., Pall, P. and Schär, C. (2013) Projections of extreme precipitation events in regional climate simulations for Europe and the alpine region. *Journal of Geophysical Research: Atmospheres*, 118(9), 3610–3626. <https://doi.org/10.1002/jgrd.50297>.
- Rajczak, J. and Schär, C. (2017) Projections of future precipitation extremes over Europe: a multimodel assessment of climate simulations. *Journal of Geophysical Research: Atmospheres*, 122(20), 10–773.
- Saaroni, H., Ziv, B., Edelson, J. and Alpert, P. (2003) Long-term variations in summer temperatures over the Eastern Mediterranean. *Geophysical Research Letters*, 30(18), 1946. <https://doi.org/10.1029/2003GL017742>.
- Schär, C., Ban, N., Fischer, E.M., Rajczak, J., Schmidli, J., Frei, C., Giorgi, F., Karl, T.R., Kendon, E.J., Tank, A.M.K., et al. (2016) Percentile indices for assessing changes in heavy precipitation events. *Climatic Change*, 137(1–2), 201–216. <https://doi.org/10.1007/s10584-016-1669-2>.
- Schär, C., Vidale, P.L., Lüthi, D., Frei, C., Häberli, C., Liniger, M.A. and Appenzeller, C. (2004) The role of increasing temperature variability in European summer heatwaves. *Nature*, 427(6972), 332–336. <https://doi.org/10.1038/nature02300>.
- Schmidli, J., Goodess, C., Frei, C., Haylock, M., Hundecha, Y., Ribalaygua, J. and Schmith, T. (2007) Statistical and dynamical downscaling of precipitation: an evaluation and comparison of scenarios for the European Alps. *Journal of Geophysical Research: Atmospheres*, 112(D04105). <https://doi.org/10.1029/2005JD007026>.
- Sillmann, J., Kharin, V., Zwiers, F., Zhang, X. and Bronaugh, D. (2013) Climate extremes indices in the CMIP5 multimodel ensemble: part 2. Future climate projections. *Journal of Geophysical Research: Atmospheres*, 118(6), 2473–2493. <https://doi.org/10.1002/jgrd.50188>.
- Smirnov, N. (1948) Table for estimating the goodness of fit of empirical distributions. *The Annals of Mathematical Statistics*, 19(2), 279–281. <https://doi.org/10.1214/aoms/1177730256>.
- Stepanek, P., Zahradníček, P., Farda, A., Skalák, P., Trnka, M., Meitner, J., Rajdl, K., et al. (2016) Projection of drought-inducing climate conditions in the Czech Republic according to Euro-CORDEX models. *Climate Research*, 70(2–3), 179–193. <https://doi.org/10.3354/cr01424>.
- Stocker, T., Qin, D., Plattner, G., Tignor, M., Allen, S., Boschung, J., Nauels, A., Xia, Y., Bex, V., and Midgley, P. (2013). IPCC, 2013: Climate Change 2013: The Physical Science Basis. Contribution of Working Group I to the Fifth Assessment Report of the Intergovernmental Panel on Climate Change, 1535 pp.
- Van der Linden, P. and Mitchell, J. (2009) *ENSEMBLES: Climate Change and its Impacts: Summary of Research and Results from the ENSEMBLES Project*. UK: Met Office Hadley Centre FitzRoy Road Exeter, p. 160.
- Vautard, R. (2013). The simulation of European heat waves from an ensemble of regional climate models within the EURO-CORDEX project. 41:2555–2575. <https://doi.org/10.1007/s00382-013-1714-z>
- Viterbo, P., Beljaars, A., Mahfouf, J.-F. and Teixeira, J. (1999) The representation of soil moisture freezing and its impact on the stable boundary layer. *Quarterly Journal of the Royal Meteorological Society*, 125(559), 2401–2426. <https://doi.org/10.1002/qj.49712555904>.
- Wang, Y., Leung, L.R., McGregor, J.L., Lee, D.-K., Wang, W.-C., Ding, Y. and Kimura, F. (2004) Regional climate modeling:

- progress, challenges, and prospects. *Journal of the Meteorological Society of Japan Series II*, 82(6), 1599–1628. <https://doi.org/10.2151/jmsj.82.1599>.
- Yan, Z., Jones, P., Davies, T., Moberg, A., Bergström, H., Camuffo, D., Cocheo, C., Maugeri, M., Demarée, G., Verhoeve, T., et al. (2002) Trends of extreme temperatures in Europe and China based on daily observations. *Climatic Change*, 53, 355–392. <https://doi.org/10.1023/A:1014939413284>.
- Zhang, X., Alexander, L., Hegerl, G.C., Jones, P., Tank, A.K., Peterson, T.C., Trewin, B. and Zwiers, F.W. (2011) Indices for monitoring changes in extremes based on daily temperature and precipitation data. *WIREs: Climate Change*, 2(6), 851–870. <https://doi.org/10.1002/wcc.147>.

**How to cite this article:** Cardell MF, Amengual A, Romero R, Ramis C. Future extremes of temperature and precipitation in Europe derived from a combination of dynamical and statistical approaches. *Int J Climatol*. 2020;40:4800–4827. <https://doi.org/10.1002/joc.6490>